2020

Stabilization of β-cristobalite in the SiO2-AlPO4-BPO4 system

Kathryn Doyle
Wright State University

STABILIZATION OF β-CRISTOBALITE IN THE SiO_2-$AlPO_4$-BPO_4 SYSTEM

A thesis submitted in partial fulfillment
of the requirements for the degree of
Master of Science in Material Science and Engineering

By

Kathryn Doyle
B.S.M.S.E., Wright State University 2018

2020
Wright State University

WRIGHT STATE UNIVERSITY

GRADUATE SCHOOL

December 4, 2020

I HEREBY RECOMMEND THAT THE THESIS PREPARED UNDER MY SUPERVISION BY Kathryn Doyle ENTITLED Stabilization of β-Cristobalite in the SiO_2-$AlPO_4$-BPO_4 System BE ACCEPTED IN PARTIAL FULFILLMENT OF THE REQUIREMENTS FOR THE DEGREE OF Master of Science in Materials Science and Engineering.

_____

H. Daniel Young, Ph.D.
Thesis Director

_____

Raghavan Srinivasan, Ph.D.
P.E.
Chair, Department of
Mechanical and Materials
Engineering

Committee on Final Examination:

_____

H. Daniel Young, Ph.D.

_____

Raghavan Srinivasan, Ph.D. P.E.

_____

Maher Amer, Ph.D.

_____

Barry Milligan, Ph.D.
Interim Dean of the Graduate School

ABSTRACT

Doyle, Kathryn. M.S.M.S.E Department of Mechanical and Material Science Engineering, Wright State University, 2020. Stabilization of β-Cristobalite in the SiO_2-$AlPO_4$-BPO_4 System.

Fused silica (silica glass) is transparent in the optical and near-infrared and has a low dielectric constant, making it suitable as a window material for radio frequency radiation. However, at high temperatures (>1100C), fused silica will easily creep and lose dimensional stability. Crystallized silica is much more creep resistant than fused silica. Silica crystallizes to many different structures including quartz, tridymite, and α- and β cristobalite. The only cubic polymorph, which is suitable for both optical and radio frequency transmission in polycrystalline form, is β -cristobalite. Unfortunately, this polymorph transforms to α-cristobalite at ~300C, and the volume change during this transformation drastically weakens the material. Consequently β -cristobalite cannot be used for most structural applications unless it is stabilized in the cubic β- phase. When boron phosphate and aluminum phosphate are added to the fused silica, the material crystallizes and results in a stable cristobalite. This stable cristobalite can be used in high temperature and dynamic environments. In order to better understand this stabilization process, X-ray diffraction, Transmission Electron Microscopy, and Scanning Electron Microscopy have been used to identify various polymorphic phases of SiO_2-$AlPO_4$-BPO_4 under various processing conditions.

TABLE OF CONTENTS

TABLE OF CONTENTS (Continued)

TABLE OF CONTENTS (Continued)

LIST OF FIGURES

Figure Page

LIST OF FIGURES (Continued)

LIST OF FIGURES (Continued)

LIST OF FIGURES (Continued)

LIST OF TABLES

Table Page

I. INTRODUCTION

Fused silica is used extensively due it its optical and near-infrared (IR) transparency. It also has a low dielectric constant for the radio frequency (RF) transparency. A material with a low dielectric constant, which promotes radio frequencies to pass through the material easier compared to a material with a high dielectric constant. Dielectric constants are also called relative permittivity in a material. A lower dielectric constant is desirable as it increases signal propagation velocity and allows a higher functional density. Polymeric materials typically offer lower dielectric constants than other ceramics but have a maximum use temperature which makes ceramic materials more desirable. [1]

Silica has upwards of 40 polymorphs which are variations of silica with the same chemical formula but with different crystal structures. The three main silica polymorphs are quartz, cristobalite, and tridymite. During the transitions from one polymorph to another, usually the chemical bonds do not break but shift slightly due to the vibration of the atoms upon heating. These transitions occur for fused silica to cristobalite, fused silica to tridymite, and cristobalite to tridymite, but does not occur for any of these transformations into quartz. Some phase transformations are diffusionless, such as β-cristobalite to α-cristobalite, which means that the bonds do not break, but this transition can destroy the materials structural integrity due to the large volume change. Other phase transformations such as quartz to cristobalite, are reconstructive, and tend to break bonds and reform during the transformation.

OBJECTIVE

The primary objective of this thesis was to study the ability to stabilize β-cristobalite with respect to the transformation to α-cristobalite by forming solid solutions in the SiO_2-$AlPO_4$-BPO_4 system. The objective of the work is to achieve a stable material, phase-stable and non-degrading material between room temperature and melting point. Another objective is to study the phase transformations and crystal structures when different ratios of 3 separate powders, silica, aluminum phosphate and boron phosphate, are combined and heat-treated to form a material that is optically transparent and has a relatively low dielectric constant.

BACKGROUND

Ceramics make up one of the three main categories of materials, metals, polymers and ceramics. Ceramics technology has existed for thousands of years, and recent advancements in the field have produced materials that are suitable for use in high-temperature aerospace components that require high strength and reliability.

POLYCRYSTALLINE CERAMICS

Ceramic materials are mostly heterogeneous, and contain internal phase boundaries (e.g. microstructure). Most ceramics are polycrystalline and in many cases are also multiphase. Polycrystalline is defined as materials that have high- or low-angle grain boundaries between the individual grains or crystallites.[2] They are typically opaque but can become transparent if the material is pore free and cubic.[3] The microstructure, determined by composition and processing history, can influence the mechanical, thermal, optical, thermochemical, and electrical properties of the material. Temperature has a large impact on these properties as well.

CERAMIC GENERAL CHARACTERISTICS AND PROPERTIES

Ceramics have distinct mechanical characteristics and properties. They have a wide variety of properties and mechanical performances to consider due to their various chemical structures, elements currently present, and the types of bonding within the ceramic. [4] Ceramics show little to no plastic deformation before catastrophic failure as shown in figure 1. Also in figure 1, it is seen that ceramics have a much higher modulus compared to metals and polymers. Ceramics are also known for their high strength and stiffness due to their covalent bonding, but are often brittle. Ceramics are frequently excellent electrical and thermal insulators due to low concentrations of free electrons compared to metals. [4]

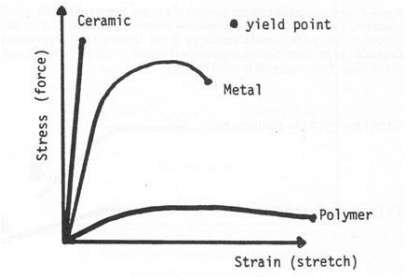

Figure 1 Stress-Strain curve of common classes of materials [5]

While there are many important chemical categories of ceramics, the classes important to this work are oxides, carbides, nitrides, silicates, and borides.

SILICATE CERAMICS

Silica, also known as silicon dioxide, has a chemical composition of SiO_2. It is the most abundant material found in the earth's crust and accounts for up to 60% of the crust. Silica can be found naturally in rocks, soil, sand, plants, animals, and even humans. [6] Silicate is a term used in chemistry to refer to a substance containing the elements of Silicon and Oxygen.

SILICA CRYSTAL STRUCTURE

All variations of silica are formed using a Si-O bond, which is the most stable bond of all Si-X element bonds. The Si-O bond has a small bond length (0.162nm) compared to the covalent radii of silicon and oxygen (0.191nm), which corresponds to the relatively high stability of the siloxane bond. [6] The three basic structures of silica are quartz, tridymite, and cristobalite. Quartz and cristobalite undergo structural changes at elevated temperatures. This transition is notated by α- or β- prefixes. The α- prefix indicates the low-temperature phase, while β- references the high-temperature phases. Quartz is the stable form of crystalline silica below 870℃, tridymite between 870℃ and 1470℃, and cristobalite between 1470℃ and 1710℃. Both of the high-temperature forms of tridymite and cristobalite can experience metastability at room temperature and atmospheric pressure without transforming into quartz. Figure 2 shows the difference crystalline and amorphous structures of silica. The crystalline structure is made up of hexagons connected with Si-O bonds which are very rigid and consistent throughout the structure. The amorphous structure is much more fluid with no real shape to each of the groupings.

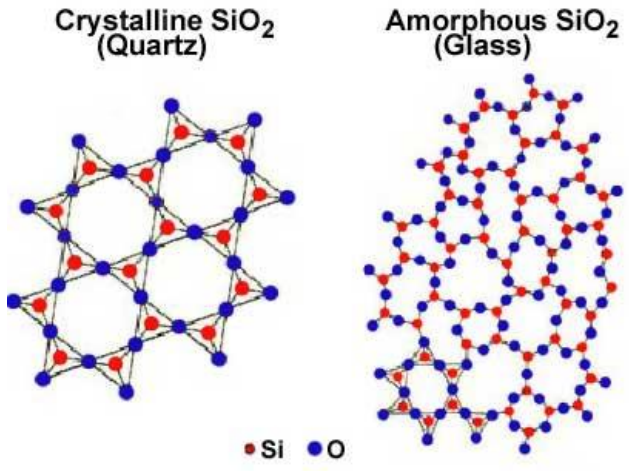

Figure 2 Crystalline and Amorphous SiO_2 structures [7]

SILICA AND ITS POLYMORPHS

Crystalline silica can be found in several different polymorphic forms which correspond to the different ways of combining tetrahedral groups with the corners shared. [8] These structures have two or three modifications that make them more or less stable at room temperature. There are also low-temperature modifications of these structures which are considered to be a derivative of the basic structure. A derivative structure is one that is distorted from a similar structure or by substitutions for its atoms by other different chemical species. [9]

FUSED SILICA

Fused silica, also known as fused quartz, is glass consisting of only silica in an amorphous or non-crystalline form, with no other additional elements. [11] Fused silica has an extremely small coefficient of expansion which makes the material thermally shock resistant. [12] If a material is prone to thermal shock, it will transform drastically as seen for cristobalite in figure 3. This property also makes it useful for precision mirror substrates. [10] Fused silica also has other important properties, such as its high viscosity which allows fibers of great strength to be drawn. Fused silica also has high transparency to ultra-violet light. [12] Figure 3 shows silica glass's extremely low coefficient of expansion compared to other silica polymorphs allowing it to withstand sudden and large temperature changes.

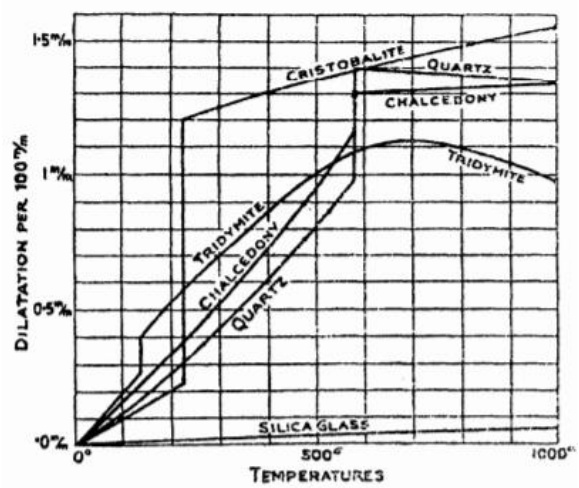

Figure 3 Expansion coefficients of silica polymorphs [13]

α-quartz has a high diffusion activation energy along with a densely packed trigonal crystal structure which is associated with the Si-O bonds within the structure. Quartz has a trigonal symmetry made up of six helices composed of the SiO_2 tetrahedra. These helices all run vertically about the central c-axis, as seen in figure 6. Although the helices have 6 sides from these helices it still has trigonal symmetry.

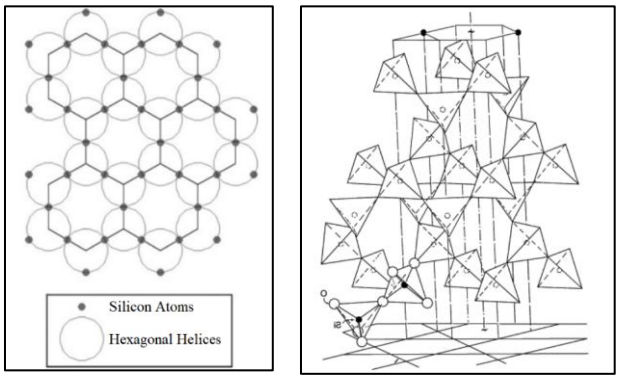

(a) (b)

Figure 4 (a) Quartz crystal structure projected on [001] plane [14] (b) *Crystal structure of quartz* [15]

POLYMORPHS

A polymorph of a substance occurs when it has the same chemical formula as the original but has a different crystal structure. For example, graphite and diamond are polymorphs of carbon. [16] There are over 40 known polymorphs of silica that have

previously been studied. [16] This paper will only discuss the temperature-dependent forms. Silica has nine network silicate polymorphs and two non-crystalline polymorphs as seen in table 1. Network silicates are all formed from a SiO_4 tetrahedron structure connected in different ways. Its two non-crystalline polymorphs are special because each silicon is surrounded by six oxygen atoms, making the packing of atoms denser, compared to the normal four oxygen atoms in a crystalline polymorph. α-variants are also known as low-variants meaning they are stable at low temperatures, while β-variants are stable at high temperatures. For α-quartz, it is stable below 573℃ while β-quartz is stable beyond 573℃.

Table 1 Silica and Non-Silica Polymorphs [16]

Silica Polymorphs (Network Silicates)	Non-Crystalline Silica Polymorphs
Quartz, Low-Quartz, α-Quartz	Stishovite
Quartz, High-Quartz, β-Quartz	Seifertite
α-Tridymite, Low-Tridymite	
β-Tridymite, High-Tridymite	
α-Cristobalite, Low-Cristobalite	
β-Cristobalite, High-Cristobalite	
Moganite	
Coesite	
Keatite	

In ambient conditions, quartz is the stable form of silica. This means that given sufficient time, all other polymorphs will eventually transform into quartz. Some polymorphs are more stable at high temperatures and pressures while others may become more stable at low temperatures and pressures. The silica polymorphs that are thermodynamically stable for pure silica are α- and β-quartz, α- and β-tridymite, α- and β-cristobalite, coesite, and stishovite. [16] Figure 3 shows the phase diagram of silica's polymorphs in terms of pressure and temperature.

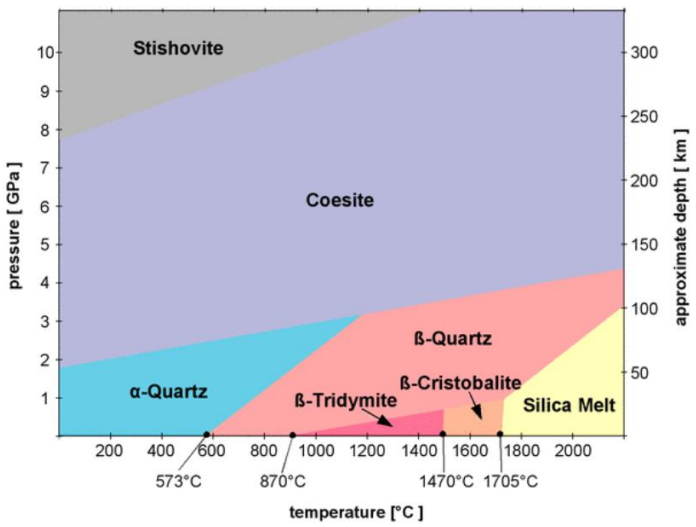

Figure 5 Phase diagram of silica [16]

PHASE TRANSFORMATION TEMPERATURES

In order for α-quartz liquify, it must transition through other phases along the way. α-quartz in its trigonal form transitions to β-quartz hexagonal at roughly 573℃. Then at 870℃, it transforms to β-tridymite hexagonal. Continuing, it transitions to β-Cristobalite at 1470℃, and then melts at 1705℃. This transition is shown in the schematic in figure 6.

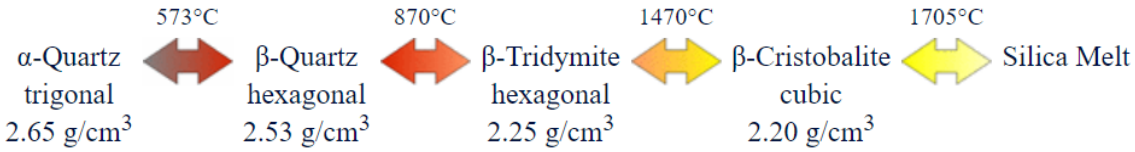

Figure 6 α-quartz transition to silica melt schematic [16]

As temperature increases, vibrations of the atoms increase in magnitude within the crystal lattice. This requires more space between atoms and results in a more open crystal structure. The open structure also depends on the geometry of the covalent bonds and its bond angles. The open structure can also alter the mechanical, electrical, thermal, and other properties. This transition from α-quartz to silica melt can be reversible if the temperature change is sufficiently slow. If the temperature changes too rapidly, it will

still transition to β-quartz from α-quartz but will then skip straight to silica melt and bypass the β-Tridymite and β-Cristobalite phases. This will also lower the melting temperature from 1705℃ to 1550℃ of the Silica melt. Once at the Silica melt phase, it can be cooled to roughly 1000℃ to form Silica glass. Glasses and melts both exhibit short-range order. Some forms of Silica show both long-range and short-range order and are seen as crystalline phases. [17]

QUARTZ

When silica transitions from α-quartz to β-quartz, the transition is displacive, meaning that the atom's positions are slightly adjusted due to the atomic movement and vibrations of the atoms upon heating. The chemical bonds are topologically displaced. As the Si-O-Si bonds become straighter the higher temperature polymorphs have a higher symmetry compared to the low-temperature counterparts. Hexagonal crystal structure corresponds to β-variants, which also generally have higher symmetry than trigonal and triclinic. [17] Trigonal and triclinic mainly correspond to α-variants. Trigonal is more symmetric than triclinic, while cubic is more symmetric than tetragonal. When this occurs, the bonds in the crystal structure are broken and then reconnected, altering the crystal structure. This is referred to as reconstructive. Quartz has a desired low dielectric constant (about 4.5) and a thermal expansion of 10-12ppm/℃ but experiences a displacive phase transformation at 573℃. This causes a large volume change which results weakening of the structure causing mechanical instabilities.

CRISTOBALITE

α-cristobalite is rarely found as an individual natural mineral, it is mainly found in cavities of silica-rich volcanic rock. Cristobalite only occurs in tiny crystals, mainly

spheres as seen in figure 7. [16] These crystals rarely become larger than 1mm in diameter. Although cristobalite is considered tetragonal in structure, it is mainly found as a pseudo-cubic octahedral polymorph [16], as it does not form directly but is formed after the transition from cubic β-cristobalite. Cristobalite generally has a milky color as there are tiny cracks within the crystal that prevent transparency.

Figure 7 Cristobalite crystals formed in silica-rich volcanic rock [16]

When α-cristobalite is put under pressure of roughly 12GPa, the cristobalite X-I phase is formed. The exact atomic arrangement is still unknown to this day, but this form does constitute an important part of the silica densification process. The phase separates the low-density tetrahedral framework from the high-density octahedral polymorphs. [18]

TRIDYMITE

Like cristobalite, tridymite is more common as a component of opal than as an individual mineral and is only found as α-tridymite.[16] Opal is a form of hydrated silica but is not truly crystalline, as it lacks all forms of order within the material. [16] Tridymite undergoes structural changes upon heating which results in changes in symmetry and crystal class. Tridymite which is formed at high-temperatures keeps its high-temperature hexagonal form but has a triclinic crystal structure. This effect also

occurs in cristobalite. Figure 8 shows the X-ray diffraction (XRD) pattern for tridymite. The x-ray diffraction is in terms of 2 theta versus intensity. The height of the intensity peak is referenced to the d-spacing which can be used to define the cell parameters. The three high-intensity maxima between 20 and 30 on the 2-theta axis, labeled with arrows, are the identifying peaks when comparing to quartz and cristobalite using x-ray diffraction.

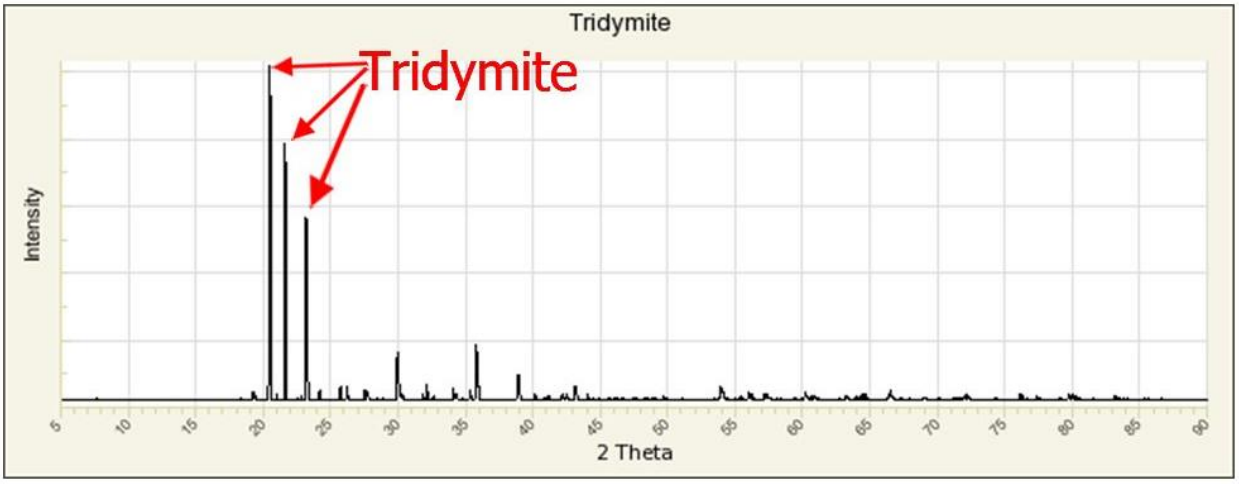

Figure 8 Tridymite x-ray diffraction pattern [19]

Figures 9 and 10 show the x-ray diffraction patterns of quartz and cristobalite respectively. In figure 9, the quartz diffraction pattern, the defining peaks for quartz are labeled.

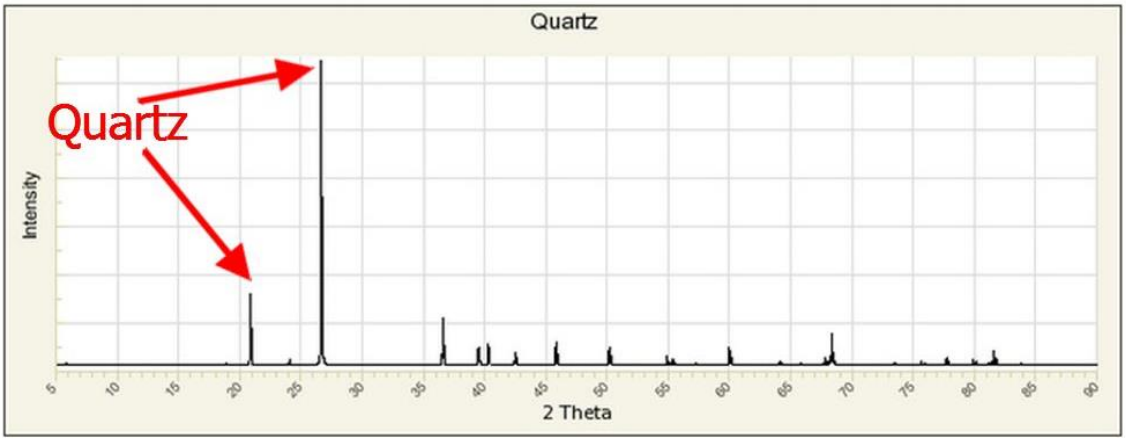

Figure 9 Quartz x-ray diffraction pattern [19]

The intensity peaks in figure 10 at roughly 22 and 36 on the 2-theta-axis refer to the cubic phases of cristobalite, labeled with a “C”. While the peaks four peaks between 20 and 40 on the 2-theta axis indicate a tetrahedral phase, labeled with a “T”.

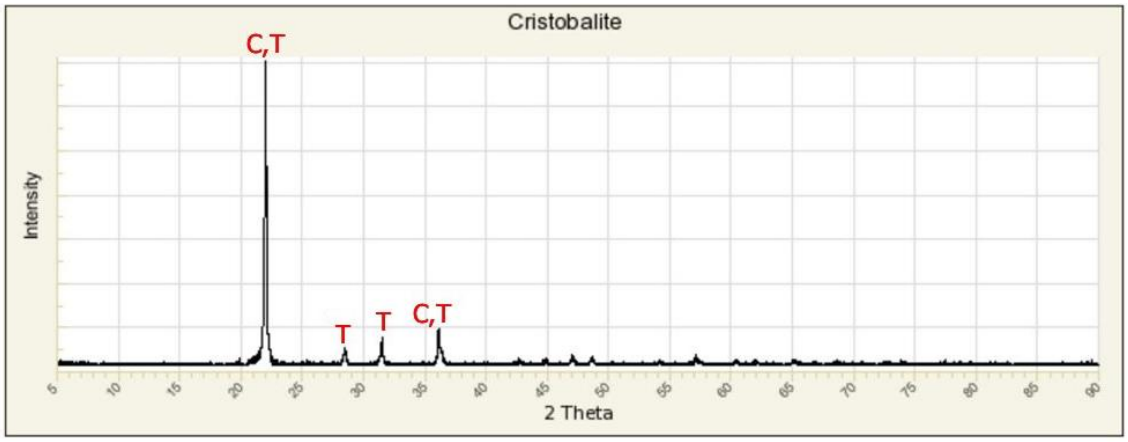

Figure 10 Cristobalite x-ray diffraction pattern [19]

The different silica polymorphs are stable at separate temperatures. When Silica is combined with Aluminum Phosphate ($AlPO_4$) and Boron Phosphate (BPO_4), and heated to 1100°C, the combination creates a cristobalite silica glass with cubic and tetragonal phases.

II. METHODS

The experimental aspect of this research project began with the patent, Boron Aluminum Phosphates and Boron Aluminum Phosphosilicates for Electronic Packaging, submitted by Yung-Haw Hu. This patent was the catalyst that prompted the examination of combining silicon dioxide (SiO_2), aluminum phosphate ($AlPO_4$), and boron phosphate (BPO_4). The patent evaluated the crystallinity over different ratios of the powders and heat treatments, and included a ternary diagram of stability of cristobalite at room temperature. The shaded regions of the ternary diagram, A_1 and A_2, indicate the compositions of β-cristobalite determined by x-ray diffraction. While the A_1 region is the

most preferred β-cristobalite compositions. Section B indicates compositions that show x-ray diffraction patterns of both β-cristobalite and BPO_4, but also shows more α-cristobalite phases, making these compositions less desirable. The ternary diagram is shown in figure 11 with indications of the various compositions that were formulated for this research project. The compositions are broken down by ratios in tables 3 and 4.

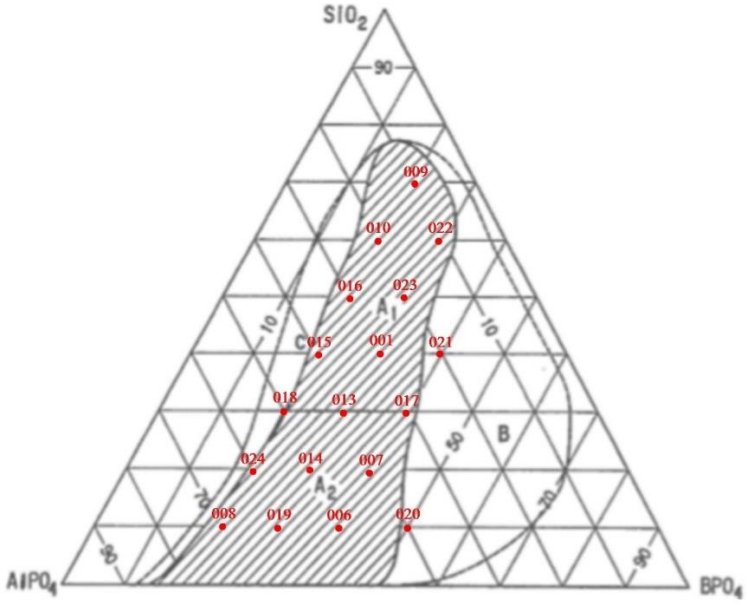

Figure 11 Ternary diagram used to pick compositions [20]

The experimental part of this project focused on mixing the 3 separate powders into a homogenous state and using thermal treatment to consolidate and homogenize.

Silica, boron phosphate, and aluminum phosphate were purchased from Sigma-Aldrich. The Silica that was purchased was LUDOX Tm-50 colloidal silica, with 50 wt% silica suspension in water. This will be referred to as LUDOX silica throughout the rest of this paper.

DEVITRIFICATION

Devitrification occurs when a glassy substance transforms into a crystalline solid. This process can be very slow (millions of years) but is why very old glassy rocks are

hard to find in nature. [21] According to Fleming, potassium is the fastest chemical element that promotes devitrification while sodium is the second-fastest. [22] This suggests that fused quartz might be slow to vitrify, since it consists of solely silicon and oxygen. Furthermore, fused quartz also has a very low hydroxyl (OH) concentration. This slows down devitrification of quartz even further, since low hydroxyl content increases the materials' viscosity and atomic diffusivity, increasing the temperature required for rapid devitrification. [23] The addition of sodium causes silica to vitrify must faster than the other materials in this project's mixture causing inaccurate results which are explained further in detail in later sections. According to the product specification sheet supplied by Sigma-Aldrich, the LUDOX silica is not purely silica and does contain up to 0.135% of Na_2SO_4 in addition to other contaminants. [24]

PROCEDURES

The cristobalite powdered mixtures were created by a mixture of certain amounts of three separate powders which include silica (SiO_2), aluminum phosphate ($AlPO_4$), and boron phosphate (BPO_4). The ternary diagram from the patent (figure 11) was used to determine a variety of compositions to be created. The compositions were mixed, dried, pressed into quarter inch thick cylinders, heat-treated, and then analyzed by x-ray analysis, scanning electron microscopy, and transmission electron microscopy.

MIXING POWDERS

To create the quarter inch thick cylinders, referred to as pucks in this thesis, to be heat treated and analyzed, a composition ratio was chosen from the shaded region of the ternary diagram shown in figure 11. Generally, the compositions were made in 9-gram batches to ensure enough to make multiple pucks if necessary. The percentages on the

ternary diagram were be converted into volume percent and then into mass (grams) to create the correct ratios of powders. The three separate powders were weighed on a scale and then combined with 50ml of deionized water in a 200ml beaker. The solution was then stirred at roughly 150 RPM for 4 hours using a magnetic stir bar on a stir plate. The solution will become milky in color but still has the viscosity of water. During the mixing, the solution was covered with Permafilm to prevent evaporation of the water. Once the solution was well mixed, it was transferred to a tall sided 5-inch diameter petri dish. The transfer allows more surface area for the water to evaporate more quickly. The petri dish was loosely covered with aluminum foil and placed in a 120℃ oven overnight, or until the water was completely evaporated. When removed from the oven, the solution was still milky in color but had a dry cracked texture like a dry desert ground. The next step was to scrape the solid out of the petri dish and grind in a mortar and pestle until no large chunks remain. The smooth powder was then transferred into a clean alumina crucible for the next heating step. The crucible was heated to 900℃ for 15 hours with a heating and cooling rate of 10 degrees per minute. Once the powders were cooled, the powder was returned to the mortar and pestle to be reground as the powder solidifies slightly during the 900℃-heat treatment.

BURNING OFF EXCESS CARBON

This heating step burns off the excess water and carbon that was found in the solution. Figure 12 shows the stages of carbon being burned off over different time intervals.

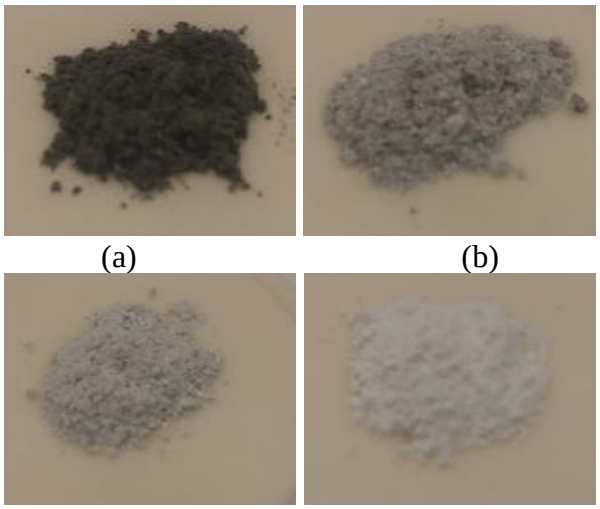

(a) (b)

(c) (d)

Figure 12 Burning off the excess carbon (a) composition 016 heat-treated at 500℃ for 15 hours. (b) composition 016 heat treated at 800℃ for 15 hours. (c) composition 016 heat-treated at 850℃ for 15 hours. (d) composition 016 heat-treated at 900℃ for 15 hours.

The carbon becomes trapped in a glass phase during the heat treatment and oxidizes into CO and CO2, causing bubbling to occur, as shown in figure 13b. With the extra carbon, the pucks also turn tan or light brown in color instead of remaining white and opaque (figure 13a).

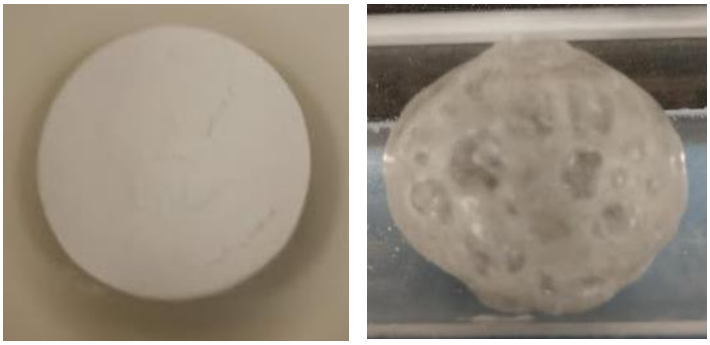

(a) (b)

Figure 13 Heat-treated compositions (a) 1100℃ for 70 hours stayed cylinder (b) 1400℃ for 1 hour with trapped gas bubbles resulting in high porosity sample

BINDER ADDITION

The next step after burning off the excess carbon was to add a binder to the solution to assist the binding capabilities during compression. Polyvinyl Butyral Resin was the binder that was used in these compositions. The new composition were 97% of

the original solution from the ternary diagram and 3% of the added binder. The powder solution and the binder were added into a clean 250ml plastic container used for ball milling, along with roughly 100 grams of alumina ball milling balls. The rest of the container was filled with isopropanol and mixed at a medium speed for 24 hours. Once the 24 hours was complete, the solution was poured through a strainer into a tall sided petri dish to separate the alumina balls from the liquid solution. The alumina balls were then sprayed with additional isopropanol to get any remaining residue off the alumina balls. The container was also sprayed with extra isopropanol to clear all remaining particles out of the container. The solution in the petri dish was covered with aluminum foil and stored in a fume hood at room temperature for multiple days, until the solution was dry. Small slits were cut into the aluminum foil to allow the isopropanol to evaporate. Now with the addition of the binder, the solution was not able to be heated to dry faster as it would burn off the binder that was previously added. Once dry, the powder was returned to the mortar and pestle one last time, pulverized until smooth. The next step was to press the powder into a 20mm diameter quarter inch thick cylinder to be heat treated.

COMPRESSING INTO QUARTER INCH THICK CYLINDERS

Using the 20mm die and ram, two grams of the smooth powder were compressed under 5000lbs of pressure using a carver tabletop laboratory press. The pressure was held for five minutes to ensure most of the air pockets were eliminated. The next step was to remove the puck from the die. This was done by suspending the die and ram an inch off the pressure plate and pressing on the ram slowly. The puck fell from the die to the pressure plate and should resemble the puck shown in figure 13a. The die should not be

suspended more than an inch above the pressure plate, as the puck could potentially crumble upon release. The next step was to heat-treat the puck.

TUBE FURNACE

Heat treatment occured in a CM incorporated rapid temp tube furnace lined with an alumina tube. A silica glass, one-inch diameter open ended tube, was placed inside the alumina tube that was suspended on each end by heat insulation alumina foam disks. The foam disks suspend the silica tube off the alumina tube for a more even heat distribution in the hot zone of the furnace. The silica glass tube also protects the puck from other contaminants that were in the alumina tube from previous experiments. The puck that was made in the previous steps was then laid on a silica glass boat made from the excess of the silica glass tubes used in the furnace. The boat was roughly 2 x ¾ inches. The puck and the boat were slid into the silica tube inside the alumina tube to be centered in the hot zone of the tube furnace.

HEAT TREATMENTS

The puck was then heat-treated in open air for 70 hours at 1100℃ with a ramp rate of 10 degrees per minute in the tube furnace. Once cooled, the puck was then cut into 4 wedges. One of the wedges was set aside for further analysis. The remaining wedges were each heat treated at 1200℃, 1300℃, or 1400℃ for 1 hour. Each separate heat treatment also had a ramp rate of 10 degrees per minute. During the 1400℃-heat treatment, the glass silica tube that was inserted inside the tube furnace began to bow from the heat. The other heat treatments did not cause any bowing to occur. The glass silica tube did experience some crystallization on the inside of the tube from the escape of gases released from the pucks during heat treatments. This occurred on all heat

treatments but was more pronounced at the higher temperatures. The crystallization is shown in figure 14.

Figure 14 Silica tube crystallizes upon heat treatment of cristobalite compositions

FABRICATING POWDER-TEOS SILICA

Due to the sodium contaminates in the LUDOX silica, Tetraethyl Orthosilicate (TEOS) was made in the lab using the following process. The powdered silica was created using the Stöber process with a high concentration of 1.115 M. [25] In a round bottom flask, which was mounted on a magnetic stir plate, controlled amounts of deionized water, Isopropanol, and trimethylamine (TEA) were added. The solution was blended with a magnetic stir bar for 10 minutes before adding the Tetraethyl Orthosilicate (TEOS) dropwise. The clear solution will begin to turn opaque as the formation of the silica suspension occurs. The solution was continuously stirred for 15 hours covered with parafilm. Next, the suspension was centrifuged at 6000RPM three separate times at 10-minute increments, replacing liquid with new isopropanol between each centrifuge step. The fourth centrifuge cycle was completed with deionized water. This last step helps clean the silica from excess carbon found in the mixture, which was identified using Fourier transform infrared (FTIR) analysis. The carbon creates issues in the later processes. The excess water was poured off, and the remaining silica solution was dried in a shallow petri dish in an oven at 120℃ for 12 hours or until dry. The silica powder was then pulverized with a mortar and pestle. The powder wass placed in an airtight

container until used in the cristobalite solutions. The following densities and molecular weights are used to calculate the concentrations of the various chemicals: ρ_{TEOS}=0.934g/cm^3, MW_{TEOS}=208.33g/mol, MW_{water}=18g/mol, $\rho_{isopropanol}$=0.7863g/cm^3, $MW_{isopropanol}$=60.10g/mol, ρ_{TEA}=.726g/cm^3, MW_{TEA}=101.19g/mol.

FABRICATING POWDER-BORON PHOSPHATE

The BPO_4 and $AlPO_4$ were analyzed using x-ray diffraction and determined that both powders from the manufacturer were both crystalline as delivered. The x-ray diffraction patterns for BPO4 and AlPO4 are shown in figures 15 and 16, respectively. For this research project, the powders need to be amorphous before mixing in order to promote low temperature homogenization, and another solution was necessary.

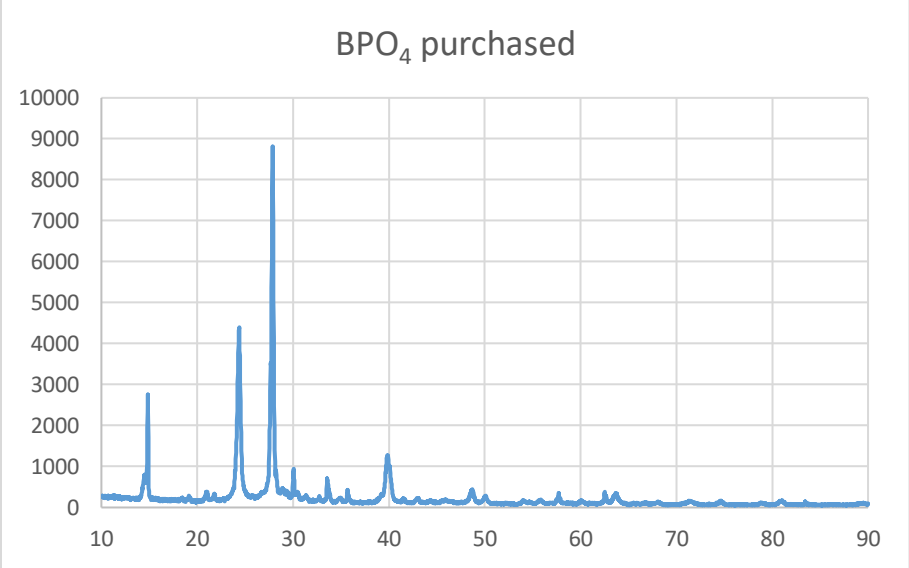

Figure 15 Plot of BPO_4 powder purchased and analyzed with X-ray diffraction

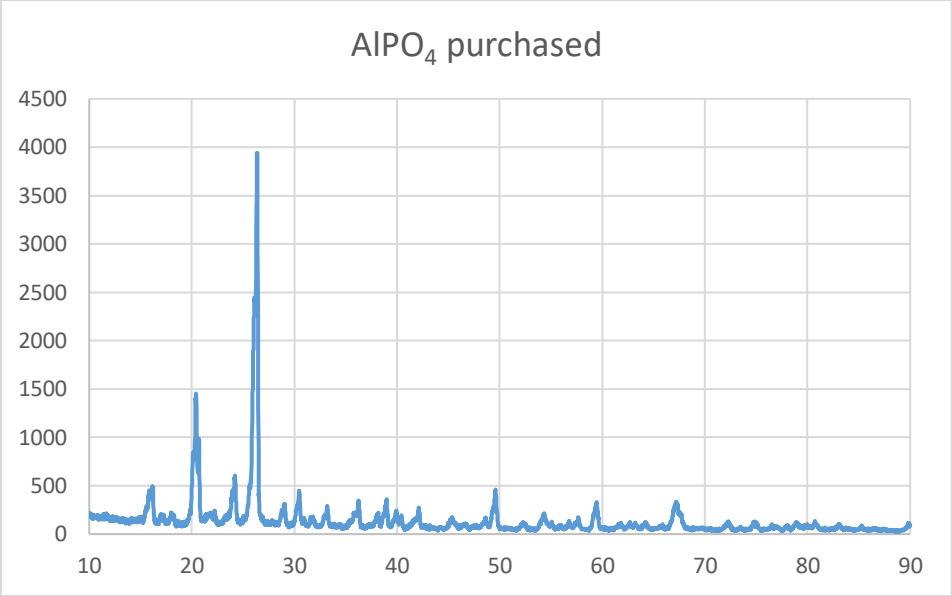

Figure 16 Plot of $AlPO_4$ powder purchased and analyzed with X-ray diffraction

Instead of making amorphous BPO_4 and $AlPO_4$, mixtures of H_3BO_3 (boric acid), H_3PO_4 (phosphoric acid), and $Al(NO_3)_3$ (alumina nitrate) were considered as additions to the silica. The H_3BO_3 and H_3PO_4 were mixed at a 1:1 molar ratio with 50 ml of deionized water or ethanol to form a low viscosity solution. [26] The solution was mixed on a magnetic stir plate uncovered for 15 hours or until only a solid remained. The humidity in the labs caused some issues with the drying process. A few different variations of this mixture were created to determine if any compositions resulted in an amorphous powder, these variations are shown in table 2.

Table 2 Compositions made to potentially make amorphous BPO_4

Sample #					
A	H_3BO_3	H_3PO_4	Deionized water	Stirred 6 hours	No heat, left in a fume hood to dry
B	H_3BO_3	H_3PO_4	Deionized water	Stirred 6 hours while heating	70C for 6 hours in fume hood
C	H_3BO_3	H_3PO_4	ethanol	Stirred 6 hours while heating	70C for 6 hours in fume hood
D	H_3BO_3	H_3PO_4	Deionized water	Stirred 6 hours	No heat, placed in a desiccator for 2 weeks

Sample A from the table became a solid which was pulverized with a mortar and pestle for analysis in the x-ray. The XRD data showed a crystalline structure in the x-ray diffraction pattern (figure 17). Samples B and C resulted in a thermal plastic-type material whereupon heating, the liquid would become a solid then while cooling, it would become a liquid again. This reaction was potentially caused by the amount of humidity in the air in the labs. After several attempts with heating and cooling, parafilm was added to the beaker while cooling, which allowed the solid to remain a solid. Sample D was placed in a desiccator under vacuum for 2 weeks. At the end of the 2 weeks, the solution had separated and created a light film floating on the water, as seen in figure 18. The floating film was extracted from the beaker and placed back in the desiccator for 2 more weeks to complete the drying process.

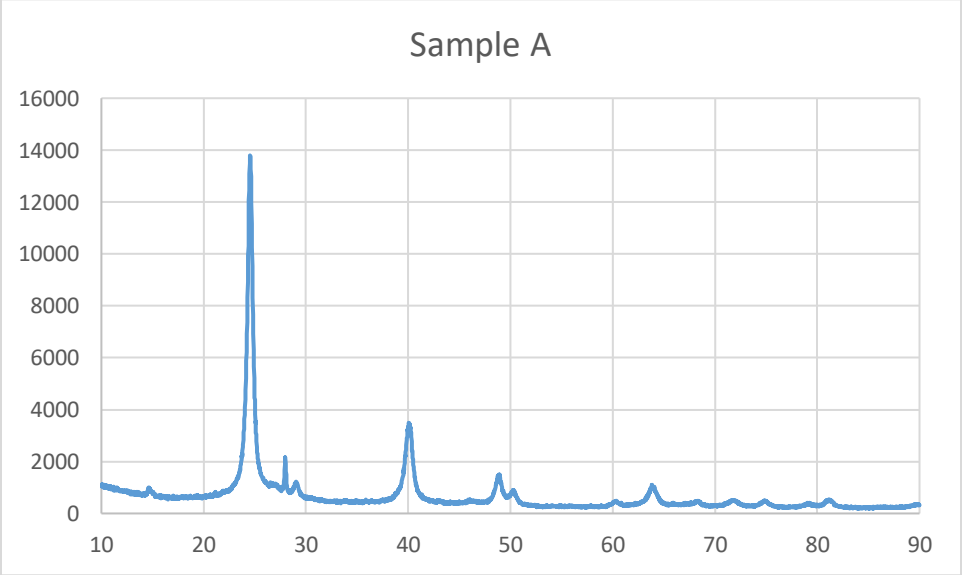

Figure 17 Plot of Sample A from table 2, no heat treatment

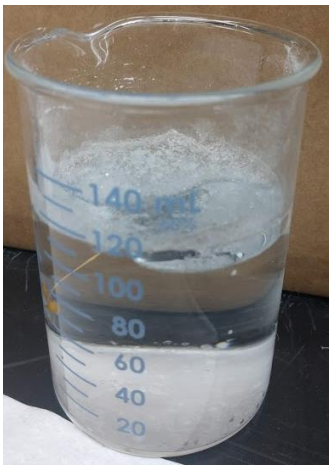

Figure 18 Sample D, created floating film while in desiccator

FABRICATING POWDER-ALUMINUM PHOSPHATE

The $AlPO_4$ can be made similarly with a 1:1 molar ratio of $Al(NO_3)_3$, H_3PO_4, and 50 ml of deionized water. The solution became a clear liquid within about 5 minutes of stirring and was stirred with a magnetic stir bar for 72 hours, it was then placed in a desiccator for further drying. After four weeks of the solution in the desiccator, the solution became a clear gel.

PREPPING FOR ANALYSIS

The wedges that were removed from the tube furnace after heating were separately put into the mortar and pestle and broken apart into fragments. Some of the fragments were saved to be analyzed in the x-ray and other microscopy techniques, while the rest of the fragments were pulverized into a powder.

The fragments were prepped for different microscopy analysis using a tripod polisher (figure 19) and lapping films on a manual metallography polishing wheel. One of the fragments from each temperature was first mounted on a Teflon disk with carbon double-sided sticky tape. Then a two-part clear epoxy was added over top to create a dome encapsulating the fragment. The epoxy was then cured in a 70°C oven for at least 4

hours, or until it becomes a dark amber color. The carbon tape attached to the fragment of the composition was then removed from the Teflon disk and attached with Crystalbond™ to a laboratory glass slide that was cut to the size of the fragment. Crystalbond™ is a thermal plastic material that upon heating melts into a liquid but upon cooling becomes a solid and bonds the sample to the glass slide. Crystalbond™ is also used to attach the glass slide with the sample onto the glass stub that was mounted into the metallography tripod polisher.

Figure 19 Tripod Polisher [27]

POLISHING

Once the samples were mounted and secured on the tripod, the sample was ready to be polished. The polishing begins with using diamond imbedded grinding disks purchased from Buehler. The disks that were used in the grinding process were, 165µm, 120µm, 70µm, 45µm, and 30µm. Once those steps were complete then the wheel was transitioned to using lapping films. The lapping films used were 30µm, 15µm, 9µm, 6µm, 3µm, 1µm, and 0.5µm. The larger the micron value was, the larger the size of the diamond particles that were embedded into the film. For example, 9µm lapping film has 9µm sized diamond particles embedded into the surface of the film that helps to slowly grind away the sample's material, this is the same for the grinding disks. To move to the

next grinding disk or polishing film, all scratches must be going in the same direction. To achieve this, the tripod was placed on the wheel so the scratches being formed were vertical on the surface of the sample, once all scratches were all the same direction, the tripod was rotated 90˚ and now the scratches will form in the horizontal direction. This ensures that the surface of the sample was all on a single plane for better analysis.

POLISHING FOR SEM

An SEM sample was created by only polishing the visible side of the sample using all the grinding pads and lapping films in the order listed previously. Once polished, the sample was roughly $1/8^{th}$ inch in thickness. The top surface had a mirror-like surface.

OPTICAL THIN SECTION

An optical thin section was created by taking the previously made SEM sample and turning the polished side down and polishing from the opposite direction. This process allows the sample to be thin and ensures that the center of the sample was being evaluated. An optical thin section was created at a thickness of about 30μm thick.

MICROSCOPE ANALYSIS-SCANNING ELECTRON MICROSCOPE

A Thermo Scientific Quanta scanning electron microscope (SEM) at Wright Patterson Air Force Base was used to evaluate the size and shape of the silica particles made during the Stöber process. Professionally made TEOS silica particles have the shape of round disks. Figure 20 shows the TEOS silica that was created in the lab and also shows disk-like shapes throughout the silica particle cluster.

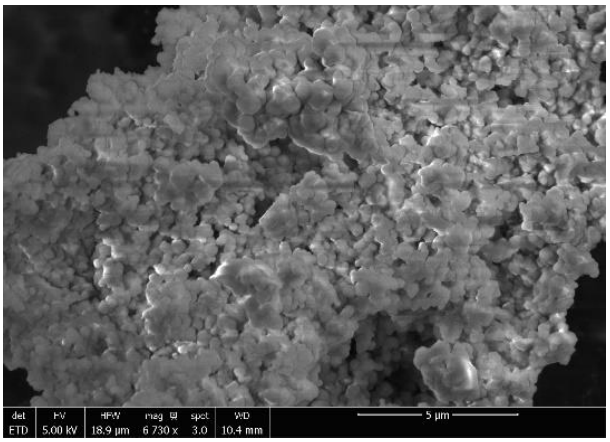

Figure 20 TEOS silica made in lab showing silica circular disk shapes

Once the TEOS silica was fabricated using the Stöber process, it was deemed necessary to determine if the TEOS silica remained amorphous over long heating times. The plot in figure 21, shows that even when the TEOS silica was heated at 700℃ for 24 hours, it remains amorphous.

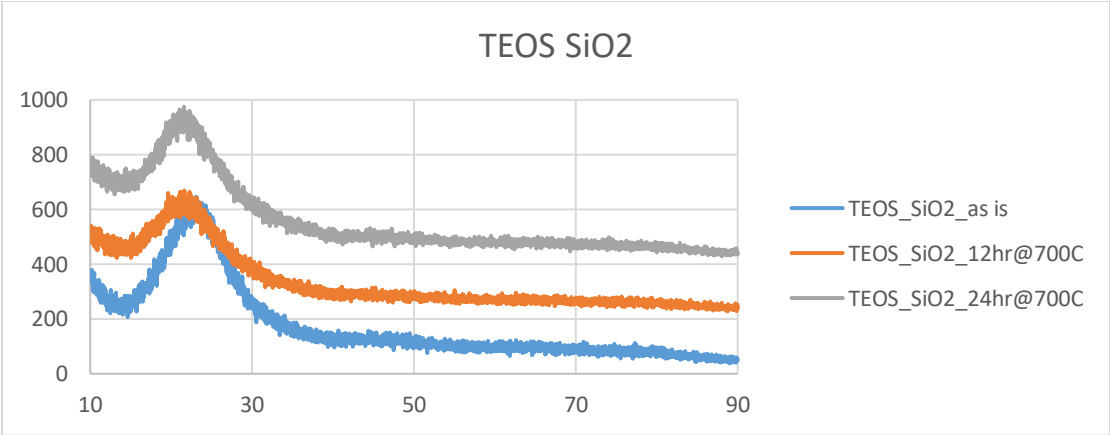

Figure 21 Plot of Amorphous TEOS silica after 700℃ heat treatments remains amorphous

Using the SEM, images were taken of the crystalline structure and impurities throughout the structure. Energy Dispersive Spectroscopy (EDS) technology in the SEM was used to determine homogenity throughout the sample. The sample did not show a homogeneous mixture throughout, meaning the powders reseparated sometime after the original mixing process, or never mixed thoroughly from the start.

MICROSCOPE ANALYSIS-OPTICAL MICROSCOPE

The optical microscope that was used in this analysis was a Nikon Optiphot. It was used to evaluate the pore size caused by either gas or air bubbles inside the sample that were trapped upon heating. One sample that was evaluated using the optical microscope, showed some stress bi-refringence which may have been caused by the polishing process. The optical microscope can also assist in determining the rough thickness across the entire sample. The thickness data was important for ion milling and for TEM analysis. Ideally, optical thin sections are roughly 2-3 um thick.

MICROSCOPE ANALYSIS-TRANSMISSION ELECTRON MICROSCOPE (TEM)

Using a Talos transmission electron microscope (TEM), images and EDS data were collected in order to characterize the interior structure of the samples. Samples were prepped in the same manner as optical thin sections, except for TEM the thickness must be about 10 nanometers, which was achieved by the ion milling process. Before the ion milling process, the samples are roughly 2-3um thick.

ION MILLING

Ion milling is an etching technique in a high vacuum chamber that uses ions of an inert gas to bombard the top surface of the sample. The ions are accelerated from a wide beam ion source onto the surface of a substrate to remove material to a desired depth. [28]

X-RAY DIFFRACTION DATA

The x-ray diffraction (XRD) data was collected on a Bruker D2 phaser. XRD is a rapid analytical technique using constructive interference of monochromatic x-rays. It is primarily used to identify the various phase of the crystalline material and it can also

provide information pertaining to the unit cell dimensions. [29] Each data set was collected over a time span of 1 hour in order to ensure ample data points. All data collected for both the pulverized and fragmented samples were collected on a zero-background holder. A zero-background holder ensures a non-destructive analytical method. The zero-background holders are made of 9N semiconductor grade silicon. The empty zero background holder was tested and is shown in figure 24 as the green data line. As shown in figure 24, sample 008 was inconclusive, as no dominant peaks show. This could be caused by a few different factors, including but not limited to the placement of the sample on the zero-background holder in the XRD machine. If the sample was not correctly placed in the center of the zero-background holder, the x-rays will impinge on the background holder and not interact with the sample. [30] When powder is analyzed with the zero-background holder, the powder must be even with the edge of the holder to ensure experimental peaks line up with the manufacturing data. The misaligned peaks may be caused by the change in lattice parameters with varying compositions.

III. RESULTS

LUDOX SILICA COMPOSITIONS

At the start of the project, as mentioned above, the powders used in the cristobalite mixtures were LUDOX silica, aluminum phosphate, and boron phosphate all purchased from Sigma-Aldrich. There was no addition of the binder added into these sample compositions as these powders bonded without assistance. A total of six different compositions were made with this powder composition. The process was explained in the mixing of powders procedure above. The list of compositions are shown in table 3.

Table 3 LUDOX Silica, $AlPO_4$, and BPO_4 compositions

Composition number	LUDOX silica	$AlPO_4$	BPO_4
001	40%	30%	30%
006	10%	50%	40%
007	20%	40%	40%
008	10%	70%	20%
009	70%	10%	20%
010	60%	20%	20%

The first mixture made from composition 001, was made with the mixed loose powder in a platinum crucible. The powder was heat-treated at 1100℃ for 70 hours in a Thermo Scientific Lindberg box furnace. When the crucible was removed, it was noted that the powder had adhered to the sides of the platinum crucible. As a consequence, forces had to be applied to remove the material. The fragments that were able to be removed were processed into optical thin sections to be analyzed under the optical microscope. The results from the optical microscope show that the sample exhibited stress bi-refringence. It is unknown what step introduced the stress bi-refringence, whether it be the breaking apart of the sample into fragmented sections, or the polishing of the sample with the grinding pads. The stress bi-refringence is shown in figure 22. Also seen in the image are large air pockets caused by gas becoming trapped in the powder during heat treatments. Some of the air pockets were caused by the powder being loose and not previously compressed prior to heat treatment.

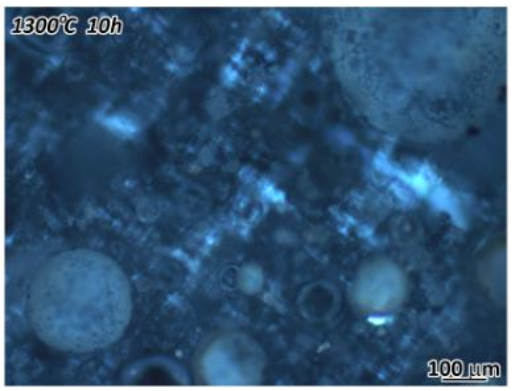

Figure 22 Stress bi-refringence

As the powder became stuck in the platinum crucible, it was determined to try cold pressing the powder into pucks to create a solid sample and also potentially prevent gas pockets from being trapped inside the material. Pucks were made of the remaining compositions listed in table 3. The box furnace was still used for these samples and the pucks were placed on alumina crucible lids. Alumina crucible material can withstand temperatures up to 1750℃ which makes it suitable for high-temperature applications. The higher temperature heat treatments, 1300℃ and 1400℃, resulted in some of the pucks becomes fused to the alumina material. Once all the compositions were pressed into separate pucks and heat-treated at the four various temperatures. The wedges were fragmented and then pulverized by a mortar and pestle to be analyzed by XRD.

LUDOX SILICA X-RAY DIFFRACTION DATA

Figures 23-30 show the XRD data collected for the LUDOX silica compositions that were left as fragments and fragments that were pulverized into a powder. Figure 23 shows the XRD data collected on the five samples made with the commercial powders that were heat-treated at 1100℃ for 70 hours. The peaks that are of interest on this x-ray diffraction pattern are located at roughly 23 and 37 on the 2θ axis. These peaks represent a cubic crystal structure.

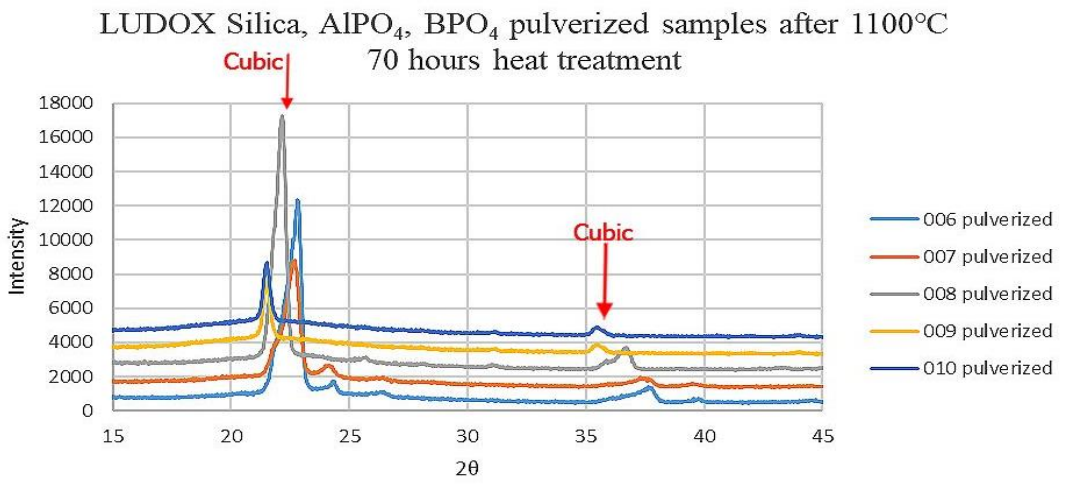

Figure 23 Plot of LUDOX Silica, $AlPO_4$, BPO_4 pulverized compositions after 1100℃ 70 hours heat treatment

The data from the fragmented pieces was much less informative compared to the data from the pulverized material. It was important for the data from the fragmented pieces to be collected due to the possibility that the material could change phase during pulverization. The sample could change phases from β-cristobalite (cubic) into α-cristobalite (tetragonal) during grinding. When comparing figures 23 and 24, none of these compositions changed from cubic to tetragonal phases but figures 25 and 26 do show some changes for three of the compositions.

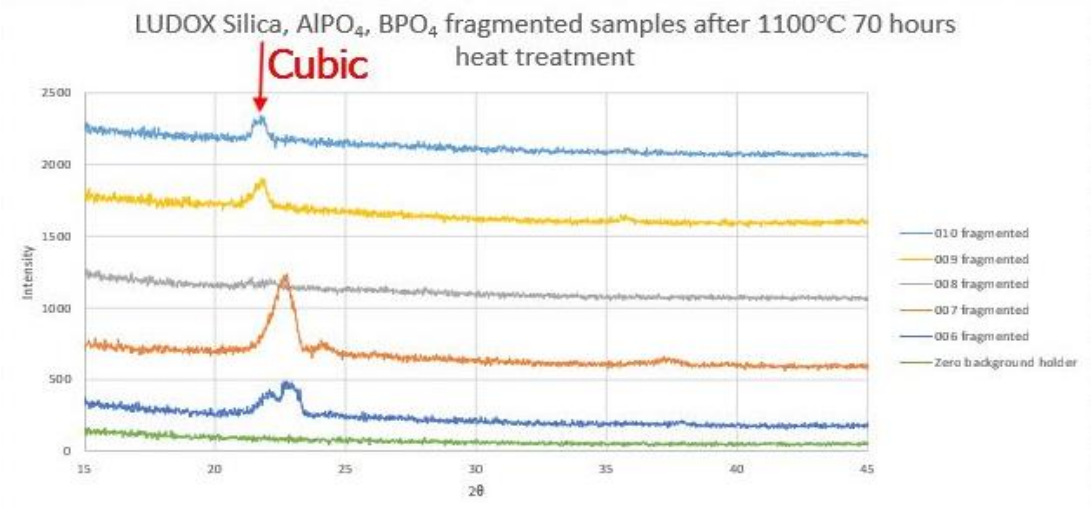

Figure 24 Plot of LUDOX Silica, $AlPO_4$, BPO_4 fragmented compositions after 1100℃ 70 hours heat treatment

Upon heat treating at 1100℃ for 70 hours and then another heat treatment at 1200℃ for an hour, composition 009 resulted in a phase transformation from cubic to tetragonal. Again, this is noted by the main 2 peaks at roughly 22 and 36 along with the smaller peaks at roughly 28 and 31, respectively.

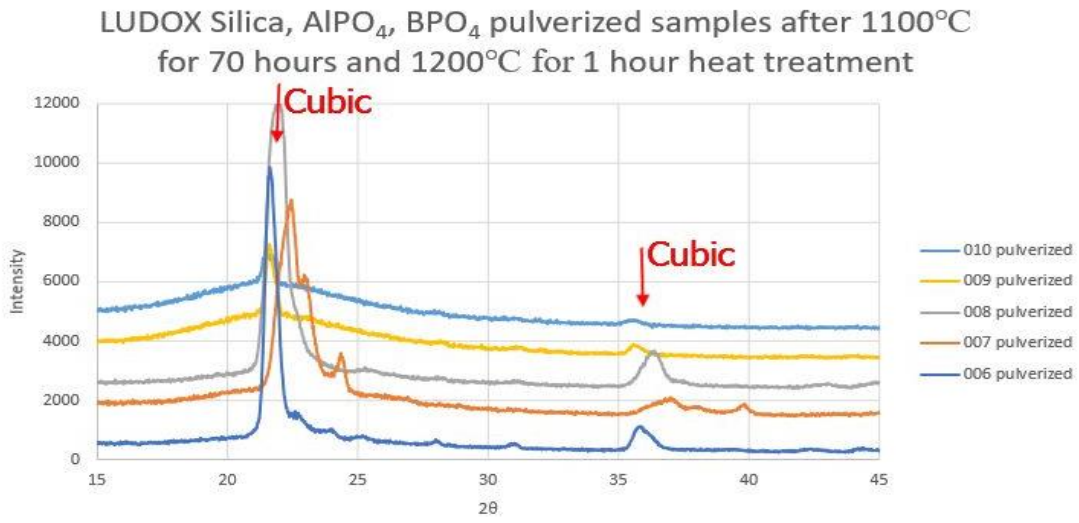

Figure 25 Plot of LUDOX Silica, $AlPO_4$, BPO_4 pulverized compositions after 1100℃ for 70 hours and 1200℃ 1 hour heat treatment

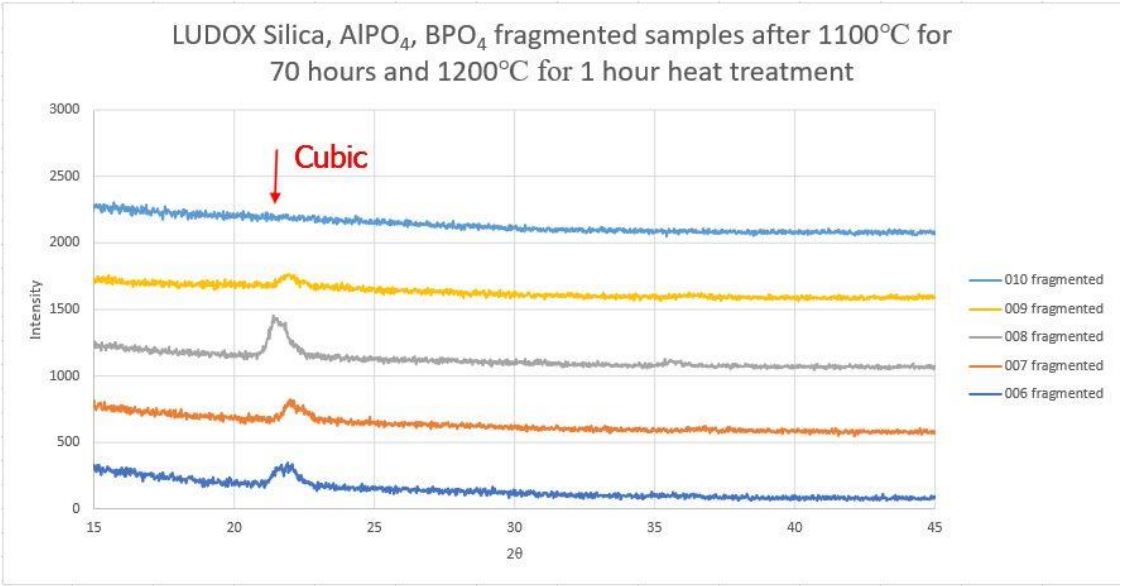

Figure 26 Plot of LUDOX Silica, $AlPO_4$, BPO_4 fragmented compositions after 1100℃ for 70 hours and 1200℃ 1 hour heat treatment

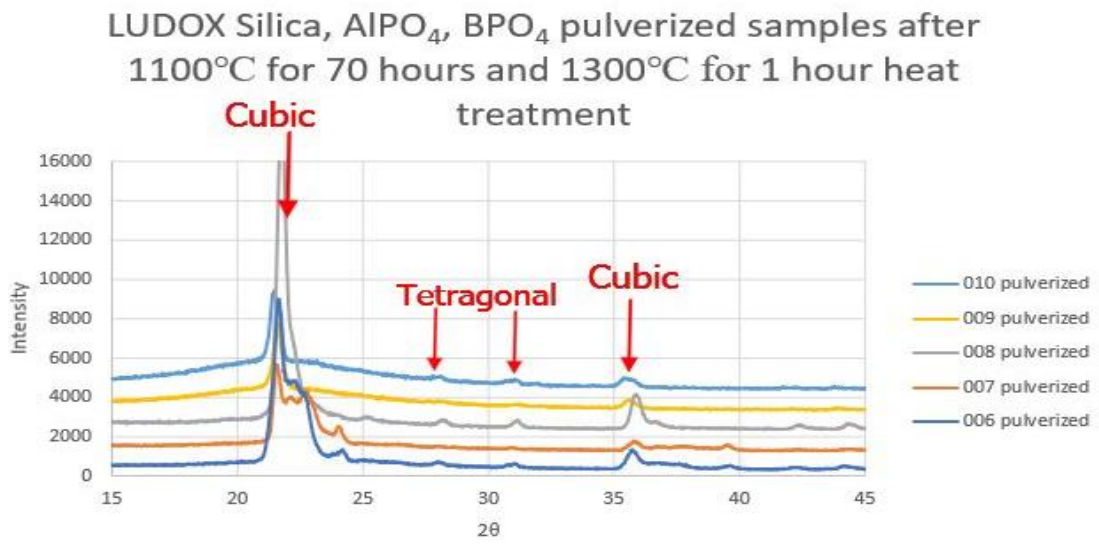

Figure 27 Plot of LUDOX Silica, $AlPO_4$, BPO_4 pulverized compositions after 1100°C for 70 hours and 1300°C for 1 hour heat treatment

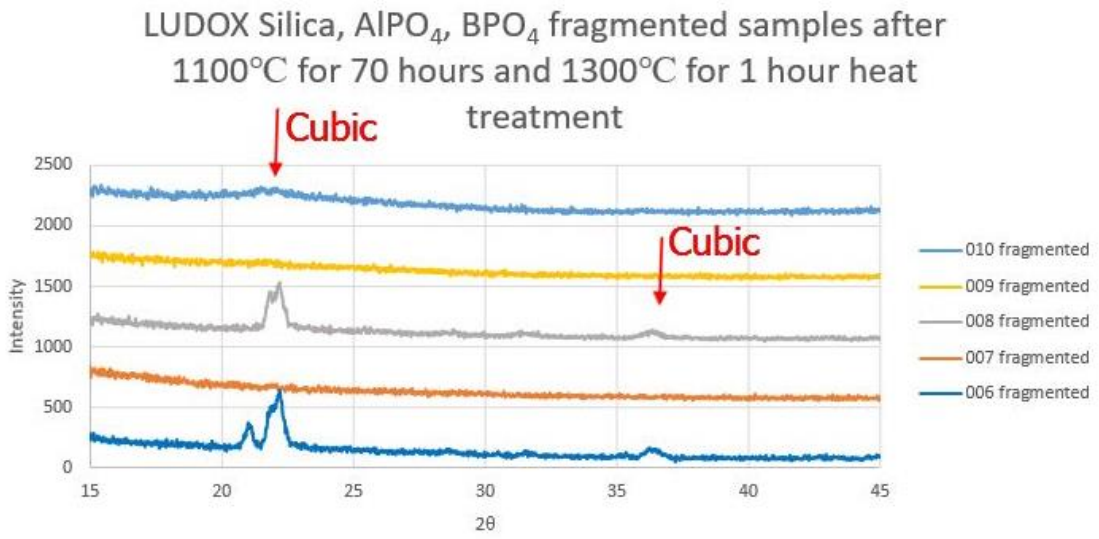

Figure 28 Plot of LUDOX Silica, $AlPO_4$, BPO_4 fragmented compositions after 1100°C for 70 hours and 1300°C for 1 hour heat treatment

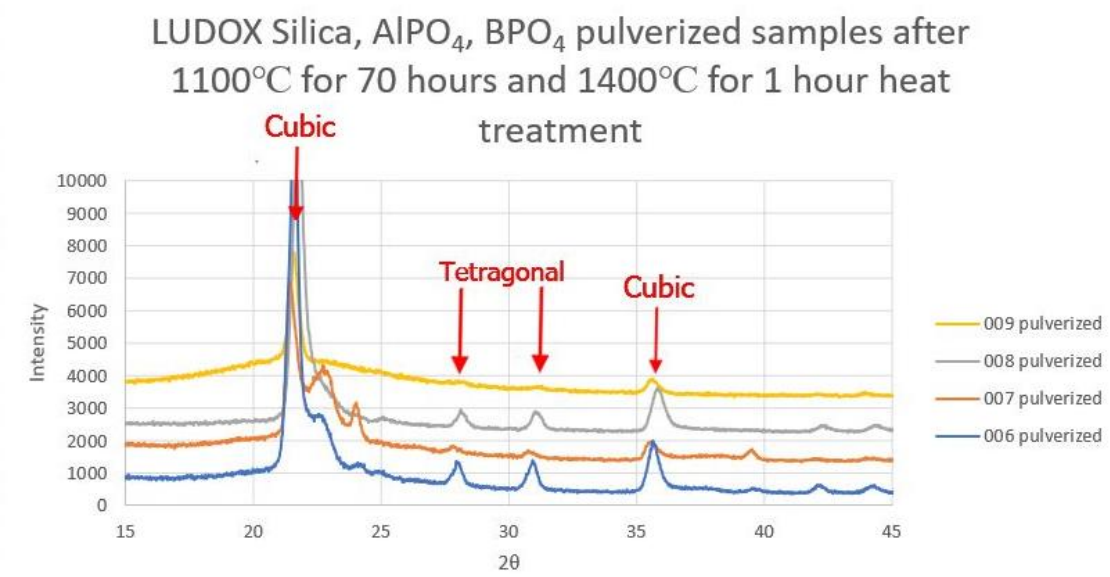

Figure 29 Plot of LUDOX Silica, $AlPO_4$, BPO_4 pulverized compositions after 1100℃ for 70 hours and 1400℃ 1 hour heat treatment

In figure 30, composition 010 shows a strong tridymite curve starting at 20 on the 2θ axis, while 007,008 and 009 were all inconclusive. Composition 006 shows that it became tetragonal when heat-treated at 1400℃ as shown in figure 30.

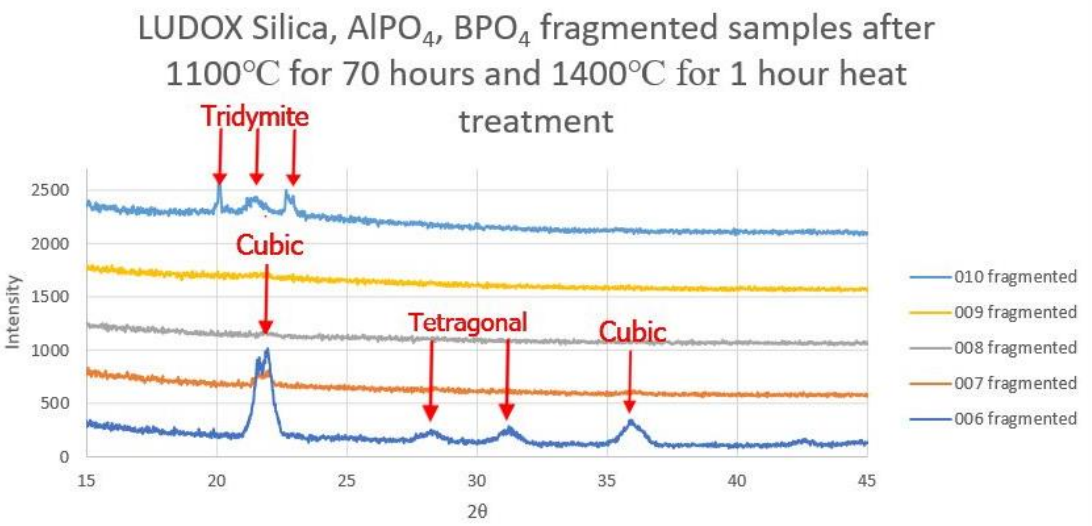

Figure 30 Plot of LUDOX Silica, $AlPO_4$, BPO_4 fragmented compositions after 1100℃ for 70 hours and 1400℃ 1 hour heat treatment

In trying to determine why some of the compositions were transforming into tridymite versus cubic or tetragonal phases, the first thought was that the box furnace that

was used for the heat treatments was contaminated with particles from other lab experiments. This led to the use of the tube furnace lined with the silica glass tube to minimize extra unknown contaminants. Changing to the tube furnace did not eliminate the tridymite phase change. That was when it was discovered that the LUDOX silica contained a small trace of sodium as mentioned before in the devitrification section. This was determined by examining the specification sheet and also creating a composition that only contained the LUDOX silica (figure 31) and not any $AlPO_4$ or BPO_4 powder. Figure 31 shows all four separate heat treatments resulted in the phase change into tridymite. Due to these undesirable data results, the fabrication of TEOS silica in the lab was deemed necessary.

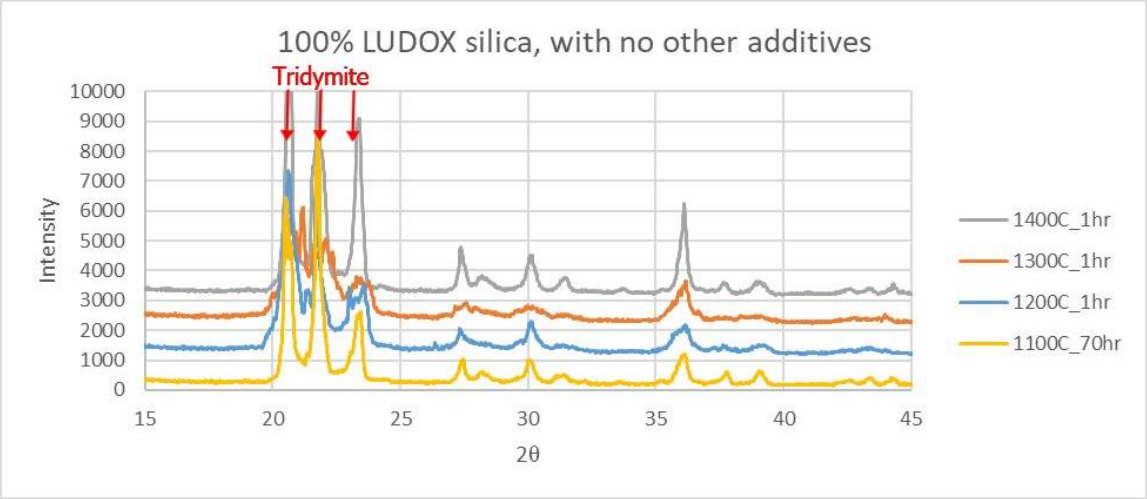

Figure 31 Plot of 100% LUDOX silica, with no other additives, compositions transforming to tridymite

TEOS SILICA COMPOSITIONS

The TEOS silica fabrication process was explained previously. The TEOS silica compositions were mixed, pressed into pucks, and heat-treated in the same way as the LUDOX silica compositions. Table 4 below lists all the compositions that were made

throughout this research project using TEOS silica instead of the LUDOX silica. Most of the compositions are within the shaded region of the ternary diagram shown in figure 11.

Table 4 TEOS Silica, $AlPO_4$ and BPO_4 compositions from ternary graph

Composition number	TEOS SiO_2	$AlPO_4$	BPO_4
001	40%	30%	30%
006	10%	50%	40%
007	20%	40%	40%
008	10%	70%	20%
009	70%	10%	20%
010	60%	20%	20%
013	30%	40%	30%
014	20%	50%	30%
015	40%	40%	20%
016	50%	30%	20%
017	30%	30%	40%
018	30%	50%	20%
019	10%	60%	30%
020	10%	40%	50%
021	40%	20%	40%
022	60%	10%	30%
023	50%	20%	30%
024	20%	60%	20%

TEOS SILICA X-RAY DIFFRACTION DATA

As the heat treatment temperatures increase, more compositions transform from β-cristobalite (cubic) to α-cristobalite (tetragonal). As stated previously, the peak shifts can be caused by the change in lattice parameters with the varying compositions.

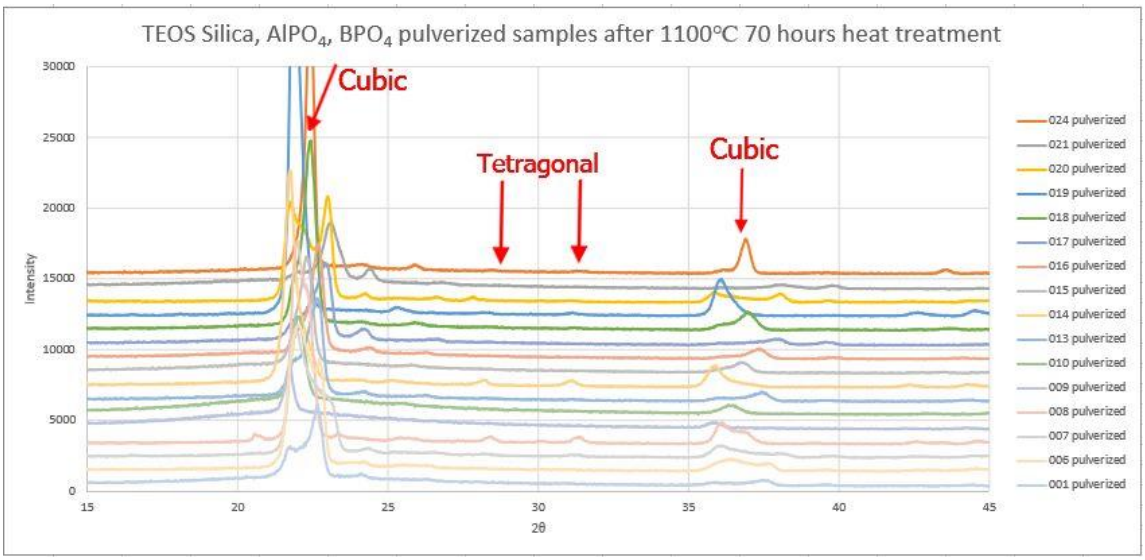

Figure 32 Plot of TEOS Silica, $AlPO_4$, BPO_4 pulverized compositions after 1100℃ 70 hours heat treatment

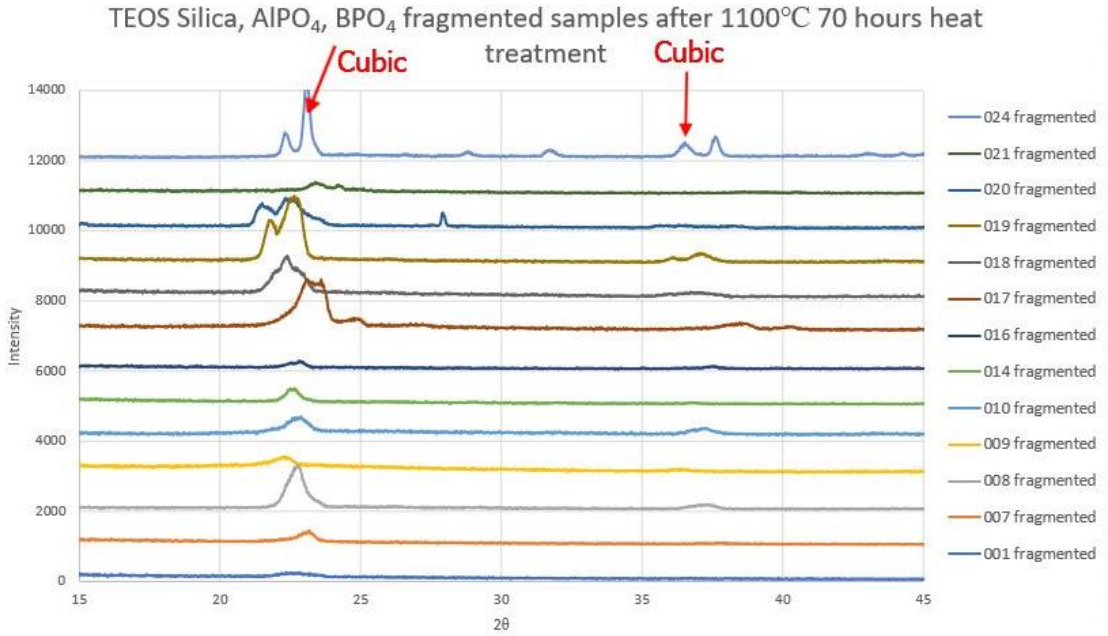

Figure 33 Plot of TEOS Silica, $AlPO_4$, BPO_4 fragmented compositions after 1100℃ for 70 hours heat treatment

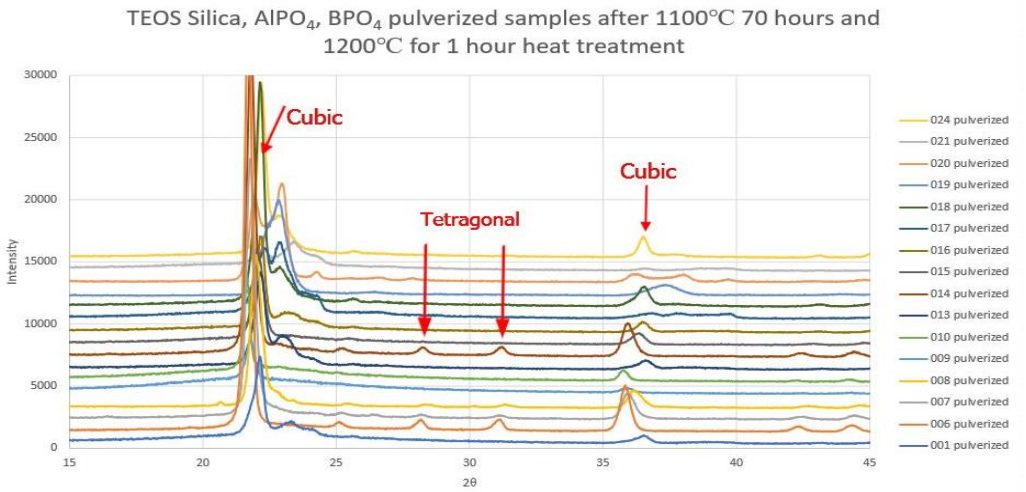

Figure 34 Plot of TEOS Silica, $AlPO_4$, BPO_4 pulverized compositions after 1100℃ for 70 hours and 1200℃ for 1 hour heat treatment

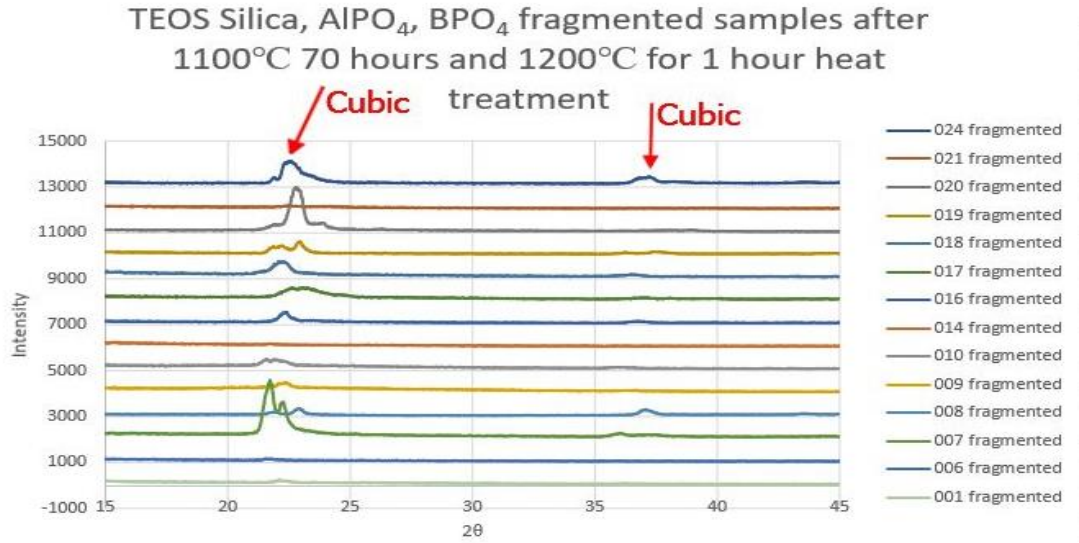

Figure 35 Plot of TEOS Silica, $AlPO_4$, BPO_4 fragmented compositions after 1100℃ for 70 hours and 1200℃ for 1 hour heat treatment

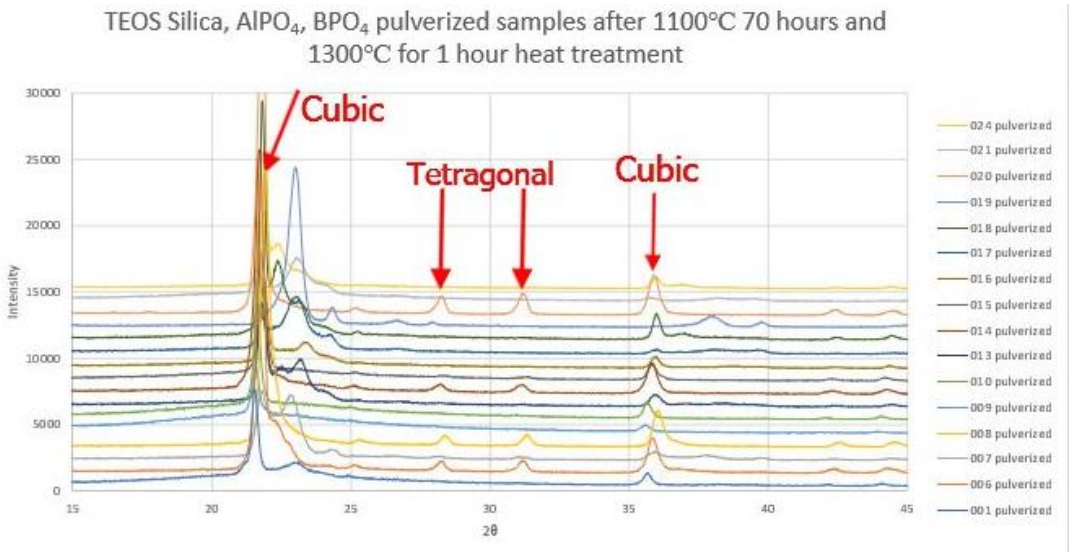

Figure 36 Plot of TEOS Silica, $AlPO_4$, BPO_4 pulverized compositions after 1100℃ for 70 hours and 1300℃ for 1 hour heat treatment

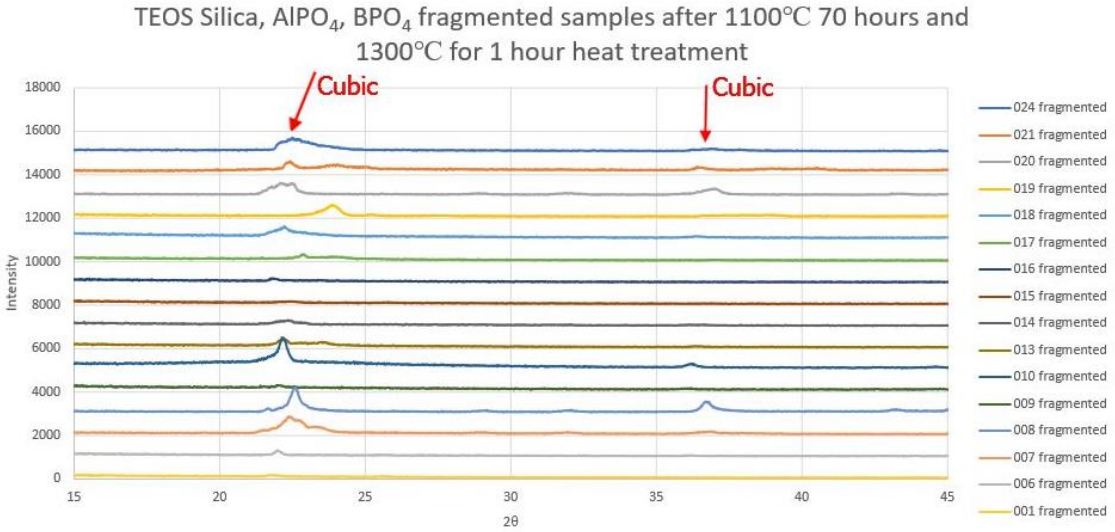

Figure 37 Plot of TEOS Silica, $AlPO_4$, BPO_4 fragmented compositions after 1100℃ for 70 hours and 1300℃ for 1 hour heat treatment

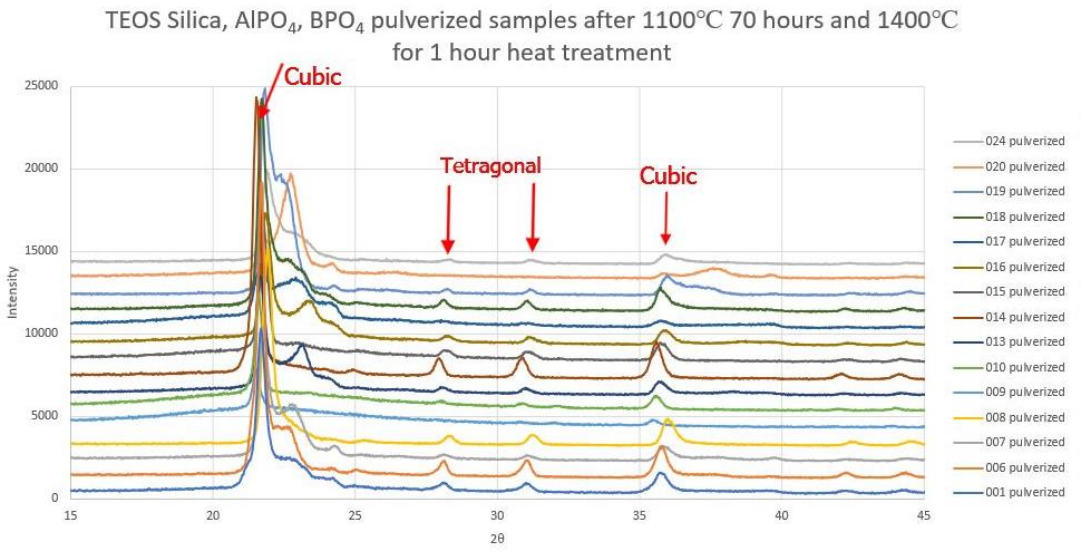

Figure 38 Plot of TEOS Silica, $AlPO_4$, BPO_4 pulverized compositions after 1100°C for 70 hours and 1400°C for 1 hour heat treatment

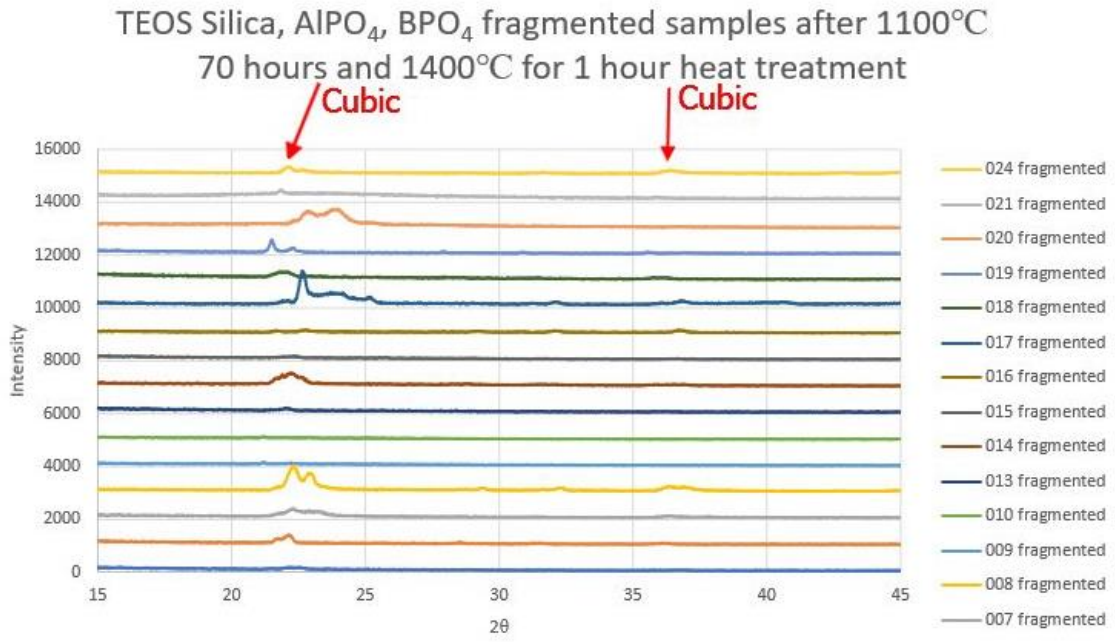

Figure 39 Plot of TEOS Silica, $AlPO_4$, BPO_4 fragmented compositions after 1100°C for 70 hours and 1400°C for 1 hour heat treatment

LUDOX AND TEOS SILICA MIXTURES

This research also included an effort to determine how sodium content affects the rate of crystallization. Compositions were created by mixing the premade TEOS silica with the LUDOX silica with 50ml of deionized water. The mixture was then dried in a

120℃ oven overnight or until dry. Then the compositions were pulverized in a mortar and pestle, then pressed with a cold press, and heat-treated in the same way as the previous LUDOX and TEOS compositions. The various compositions are listed in table 5 below. Each composition was analyzed with XRD for both pulverized and fragmented samples.

Table 5 LUDOX and TEOS Mixture compositions

LUDOX silica	TEOS silica
5%	95%
10%	90%
20%	80%
30%	70%
40%	60%
50%	50%
60%	40%
70%	30%
80%	20%
90%	10%

The data in figure 40 shows that with 50 percent LUDOX and 50 percent TEOS, the samples transition into tridymite from the cubic phase at 1100℃ heat treatment. When the composition has more than 50 percent LUDOX, the composition will result in the tridymite phase. If there was more TEOS in the solution than LUDOX, the solution will generally remain cubic or tetragonal during all heat treatments as seen in figures 40-47.

LUDOX AND TEOS SILICA MIXTURES X-RAY DIFFRACTION DATA

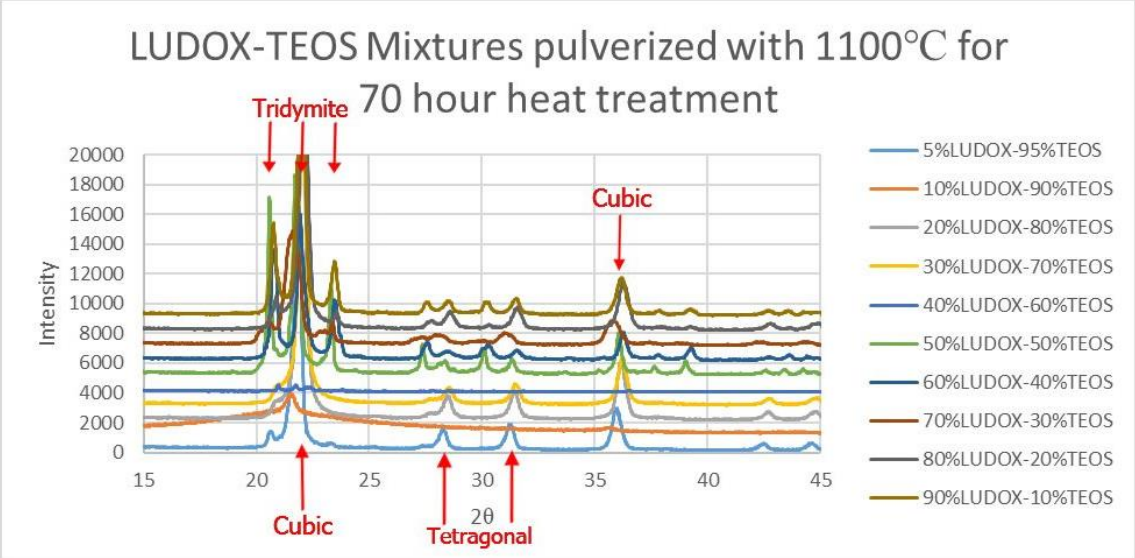

Figure 40 Plot of LUDOX-TEOS mixtures pulverized with 1100℃ for 70-hour heat treatment

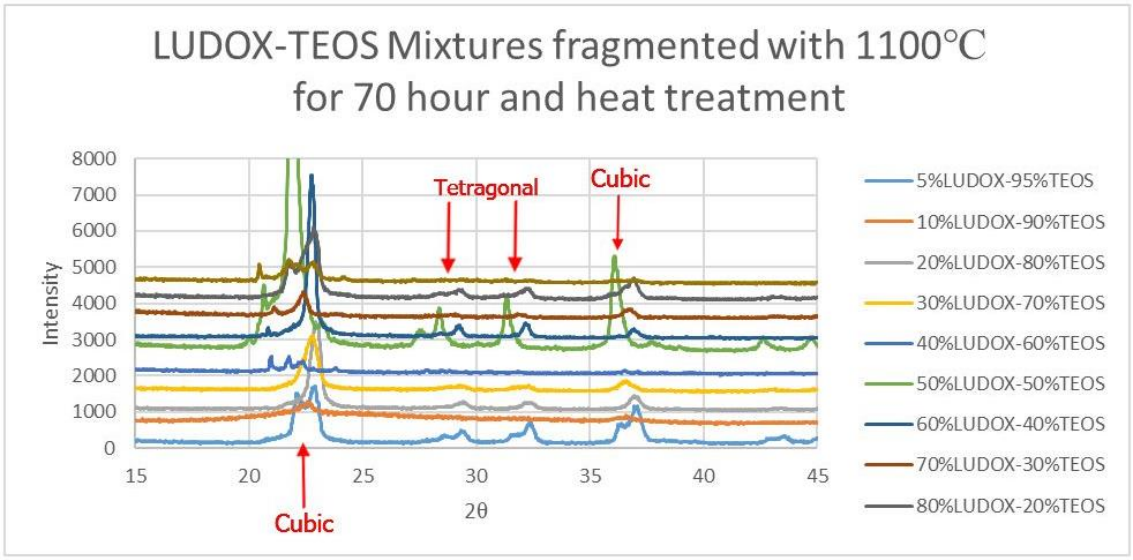

Figure 41 Plot of LUDOX-TEOS mixtures fragmented with 1100℃ for 70-hour and heat treatment

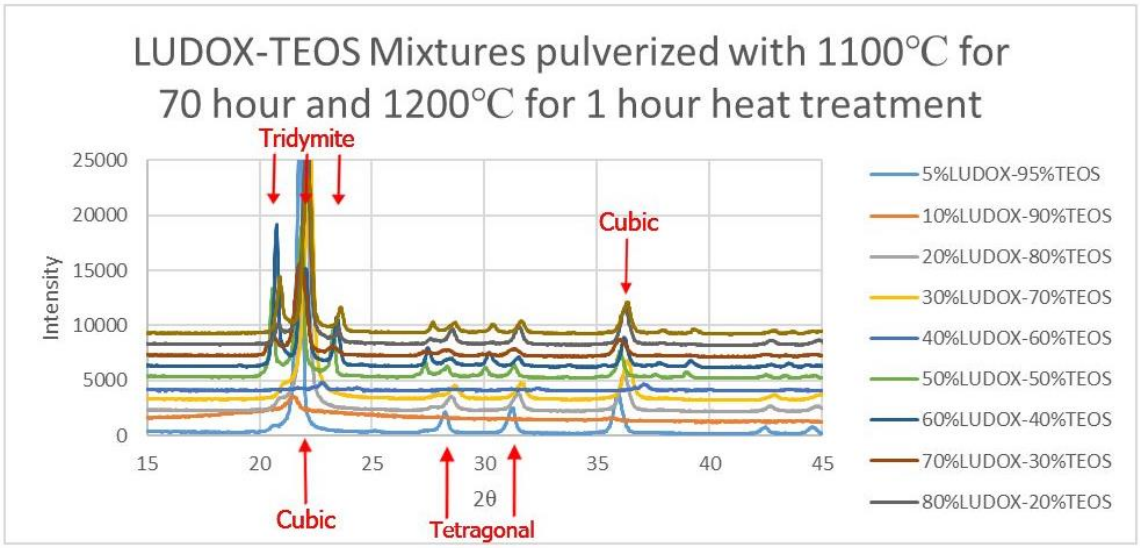

Figure 42 Plot of LUDOX-TEOS mixtures pulverized with 1100℃ for 70 hour and 1200℃ for 1-hour heat treatment

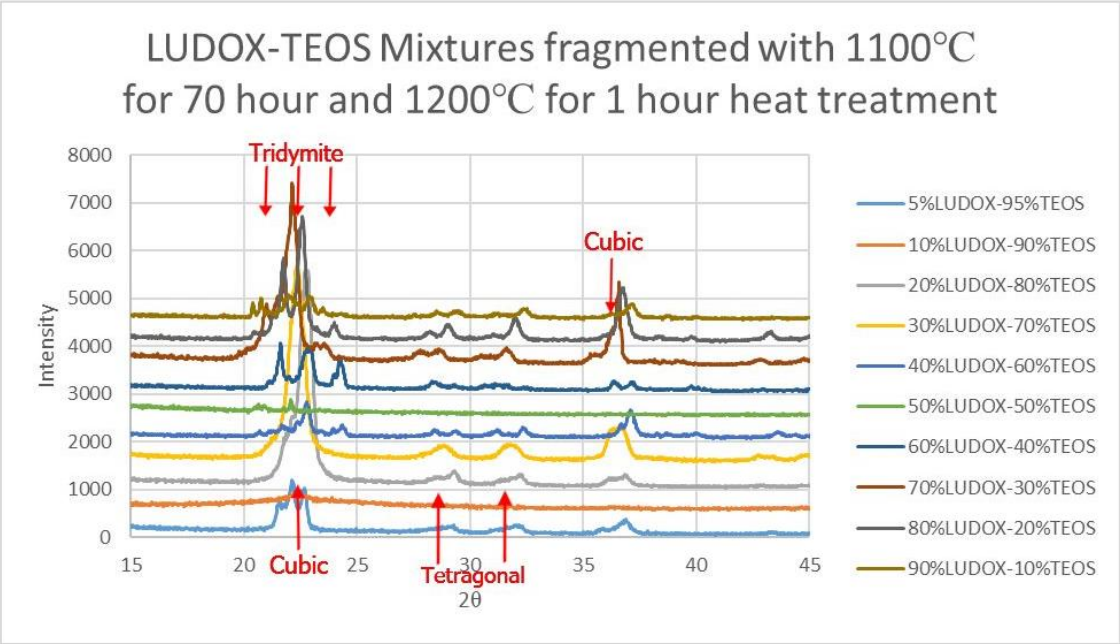

Figure 43 Plot of LUDOX-TEOS mixtures fragmented with 1100℃ for 70 hour and 1200℃ for 1 hour heat treatment

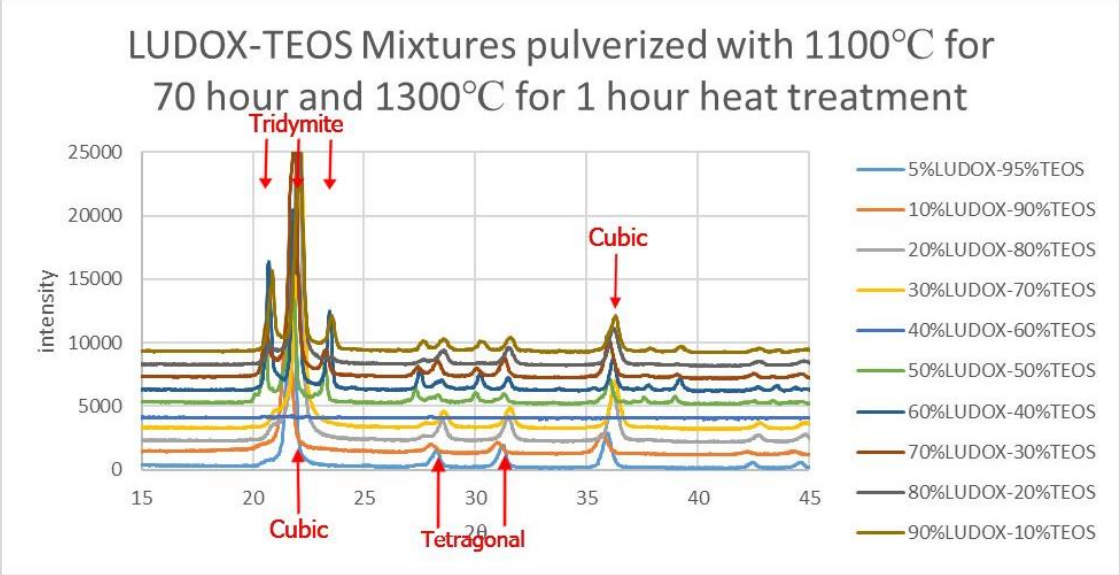

Figure 44 Plot of LUDOX-TEOS mixtures pulverized with 1100℃ for 70 hour and 1300℃ for 1 hour heat treatment

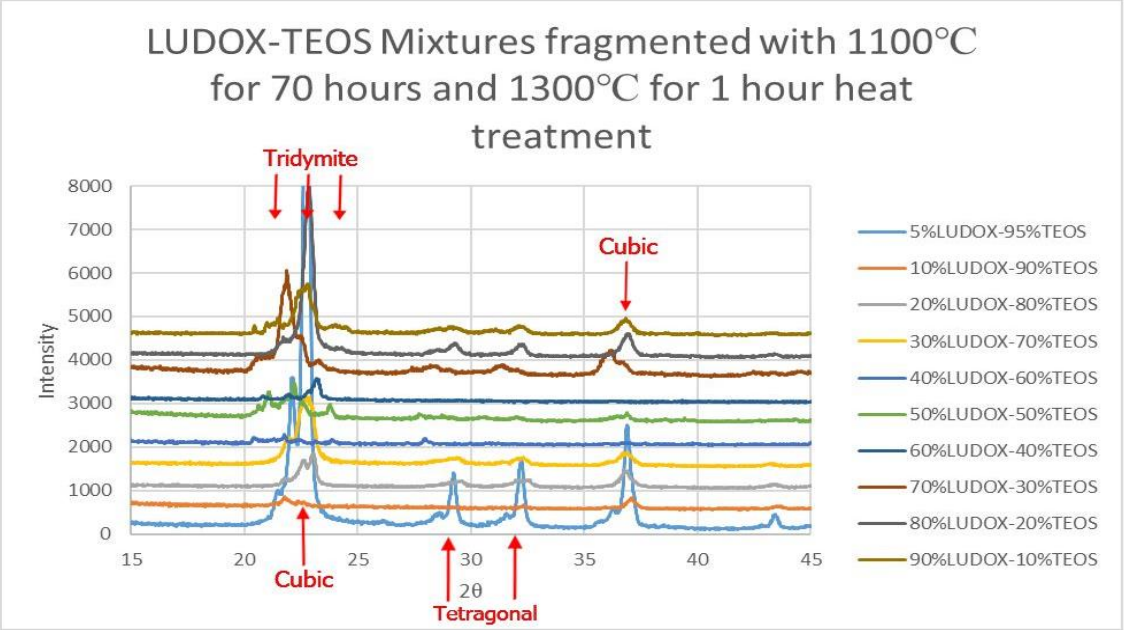

Figure 45 Plot of LUDOX-TEOS mixtures fragmented with 1100℃ for 70 hours and 1300℃ for 1 hour heat treatment

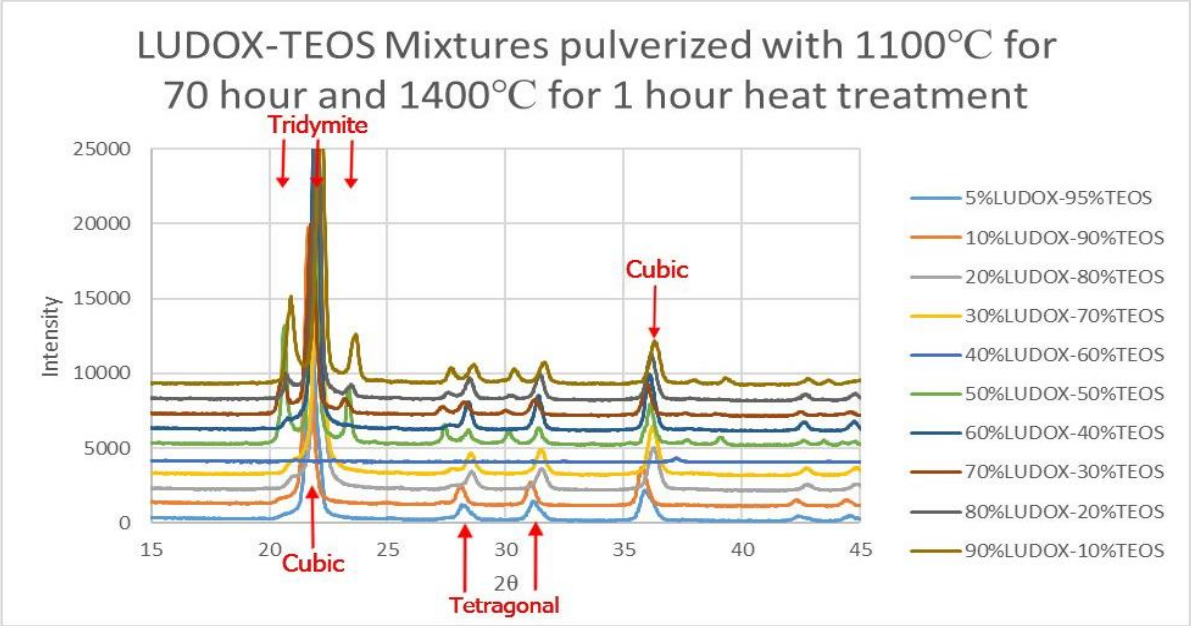

Figure 46 Plot of LUDOX-TEOS mixtures pulverized with 1100℃ for 70 hour and 1400℃ for 1 hour heat treatment

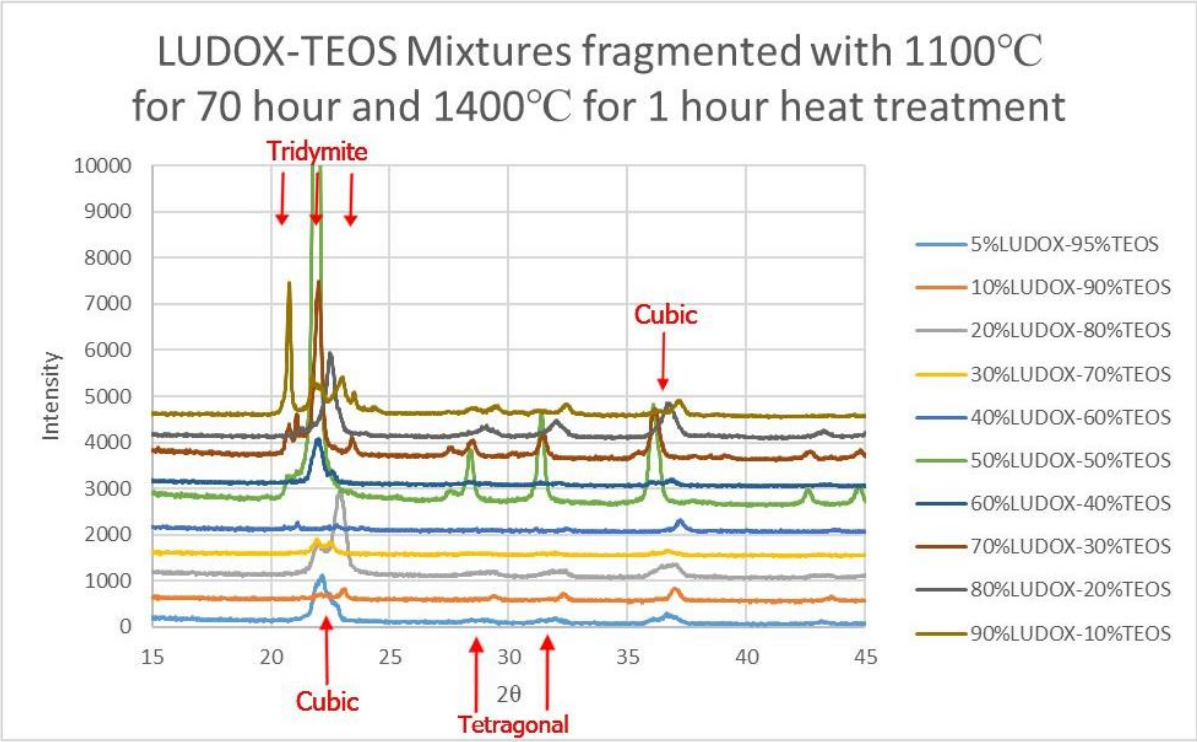

Figure 47 Plot of LUDOX-TEOS mixtures fragmented with 1100℃ for 70 hour and 1400℃ for 1 hour heat treatment

This data from the LUDOX and TEOS mixtures show that when a solution has 50 percent or more of LUDOX silica, the composition will become tridymite upon any amount of heating above 1100℃.

TRANSMISSION ELECTRON MICROSCOPY

TEM images of composition 008 (heat-treated at 1100℃ for 70 hours) are shown in figure 48a and 48b, with different phases appearing throughout the sample. Some regions showed amorphous silica while others were heavy in phosphorus. Very small and diverse regions contained all three elements together. Boron was able to be detected by the EDS for the 1100℃-heat treatment (figure 49) but were not detected in the higher temperature samples when using the same settings (figure 51).

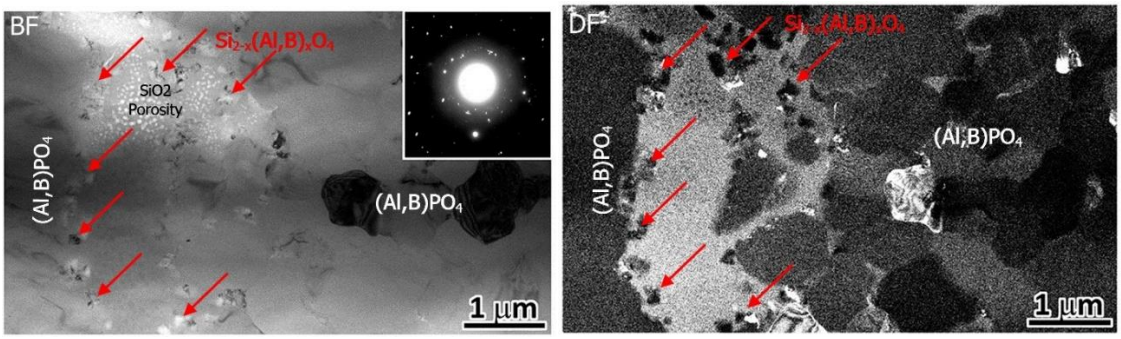

(a) (b)

Figure 48 Composition 008, heated treated at 1100℃ for 70 hours (a) Bright Field TEM image of composition containing TEOS Silica, $AlPO_4$, and BPO_4. (b) Dark Field TEM image of composition containing TEOS Silica, $AlPO_4$, and BPO_4.

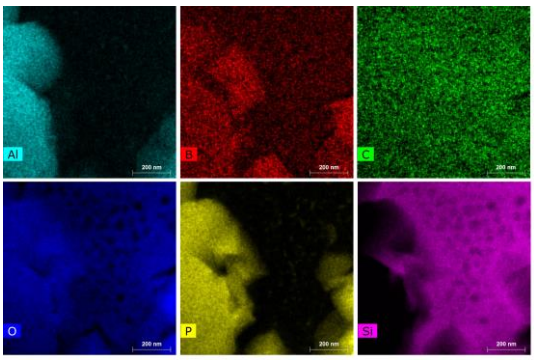

Figure 49 EDS results of sample imaged in figure 48

Figure 50 was imaged in the [111] direction and shows some twin lamella lines which occurs when two separate crystals share some of the same crystal lattice points symmetrically. [31]

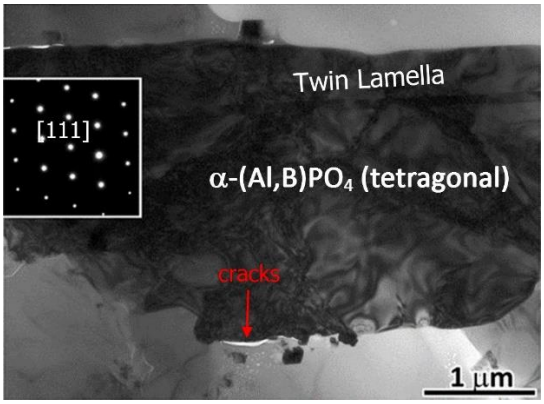

Figure 50 Composition 008 1100℃ heat treatment for 70 hours. Showing twin lamella lines and internal cracks

The second sample to be viewed in the TEM was composition 008 that was heat-treated at 1400℃. The results from the TEM also showed that multiple phases were present. It also shows that there were separate regions of amorphous silica and phosphate rich regions.

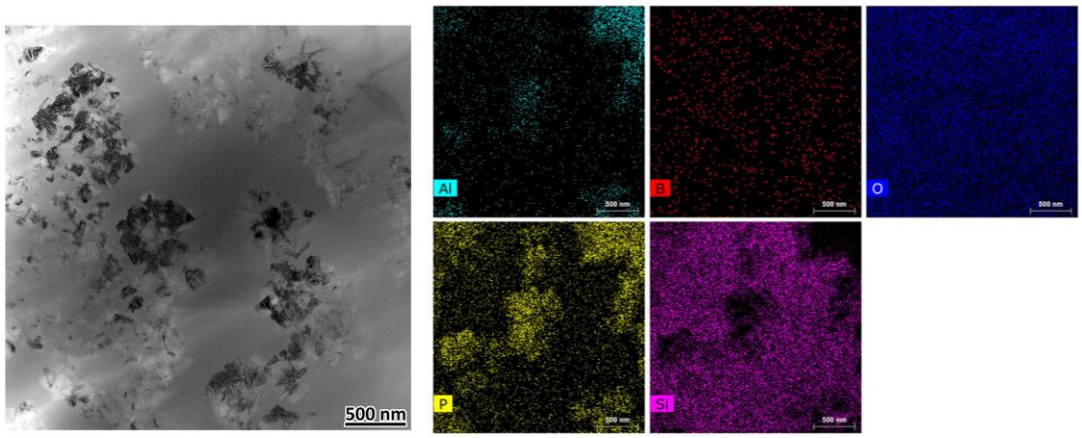

(a) (b)

Figure 51 (a) Bright field composition 008 1400℃ heat treatment (b) EDS data of figure 51

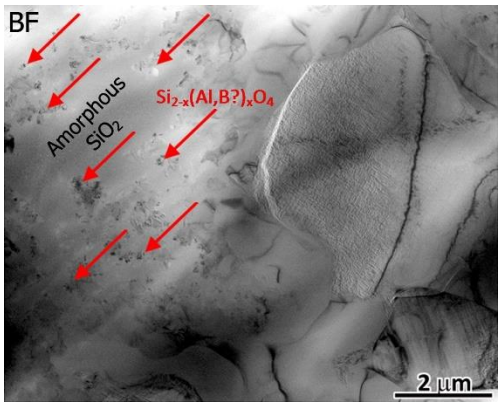

Figure 52 Composition 008 1400℃ heat treatment showing various phases in a single sample

HOT ISOSTATIC PRESSING

From the beginning, with both LUDOX and TEOS silica, all compositions that were created remained optically opaque even after heat treatments. In order to improve transparency, Hot Isostatic Pressing (HIP or hipping) was utilized. HIP is a fabrication

process in which a pre-molded shape is subjected to both high temperatures and high isostatic pressure simultaneously using a gas transfer medium. Hipping can remove both macro- and micro-porosity while not disturbing the microstructure of the material. [32] Boron phosphate has a high vapor pressure rate, which resulted in the loss of boron, leaving an excess of phosphate. HIP requires relatively lower temperatures, reducing the potential for boron loss. High porosity could be one of the factors as to why the samples that were created in this research project were optically opaque. For a sample to be processed with HIP, it must have limited to no open porosity, also known as dead-end pores, but the sample can possess closed pores. The difference between open and closed pores is shown in figure 53.

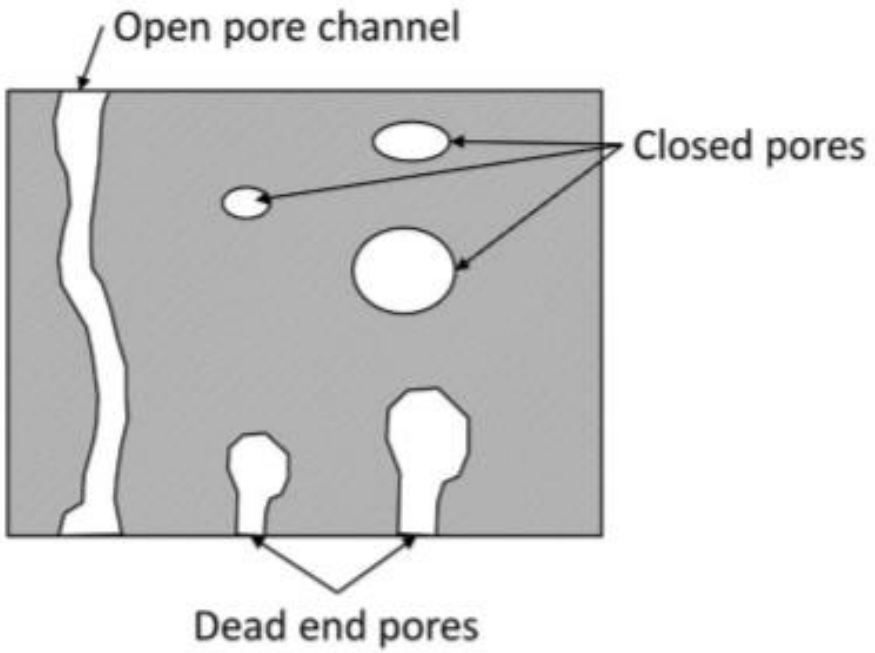

Figure 53 Open and closed porosity [33]

A total of eight samples were prepped for hipping but only four were deemed fit to be processed in that manner due to the porosity on the surfaces. This was determined by images taken on the Quanta SEM, the results of which are shown below.

COLD PRESSING

Two samples were cold pressed and heat-treated in the tube furnace were chosen to be further processed by HIP as determined by their limited open porosity compared to the other heat-treated samples. Figure 54 shows composition 008 after being cold-pressed and heat-treated at 1200℃ for 1 hour. The sample shown in figure 55a was cold-pressed and heat-treated at 1300℃ for 1 hour. During 1300℃ heat treatment, it adhered to the silica glass tube in the tube furnace and had to be forced out of the glass tube, hence the rounded shape. The SEM image in figure 55b displays a smooth non-porous surface, but the area that was broken away upon removal from the tube shows interior pores.

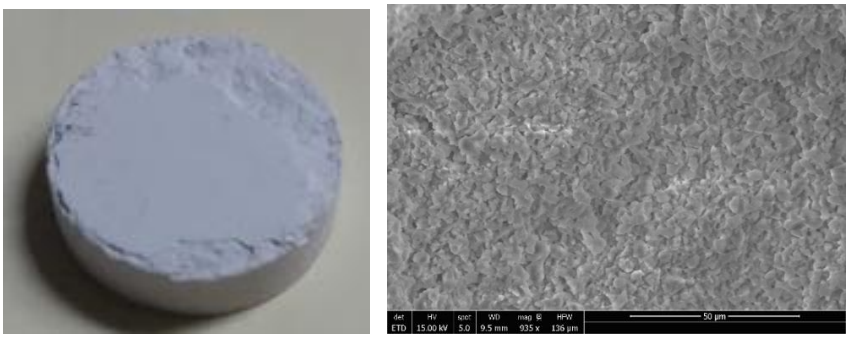

(a) (b)

Figure 54 Composition 008 made from 2 grams of loose powder (a) Composition 008 cold-pressed and heat-treated at 1200℃ for 1 hour (b) open porosity on the entire surface

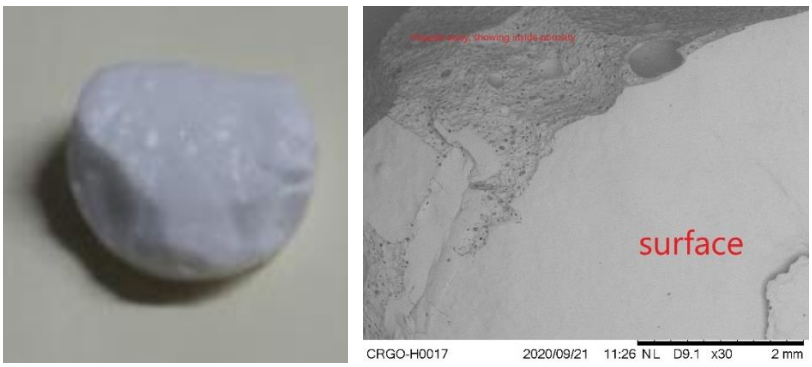

(a) (b)

Figure 55 Composition 008 made from 2 grams of loose powder (a) cold-pressed and heat-treated at 1300℃ for 1-hour (b) SEM image showing porosity only on interior but no open porosity on the surface

SPARK PLASMA SINTERING

Spark plasma sintering is a sintering method that uses a pulse of current directly passing through the graphite die as well as the powdered sample. A sample made by spark plasma sintering (SPS) was encapsulated with graphite and compressed at high temperature and pressure, and produces a near theoretical density sample. [34] Surface porosity was not able to be determined prior to hipping due to the encasing of the sample with the graphite sheets.

Figure 56 SPS composition 008 made from two grams of powder

HOT ISOSTATIC PRESSING RESULTS

The four samples were encased in a thin molybdenum film and were HIPed separately for 2 hours at 1250℃ with 30,000PSI. The list of samples that were chosen to be HIPed are shown in table 6, along with their densities prior to being HIPed. The composition 008 cold-pressed and heat-treated at 1300℃ crumbled during treatment and resulted in some fragments as large as 5mm in diameter, while the rest was powder. Composition 008 cold-pressed and heat-treated at 1200℃ stayed more intact during hipping but did have a reaction with the foil and turned part of the sample a bright purple color. SPS-001 looks the same as the non-hipped SPS sample but upon further analysis the inside of the puck turned dark black, suggesting that the graphite reacted with the sample. SPS-008 went into the HIP as shown in figure 56 but lost its graphite outer layer

during hipping. Only composition 008 cold-pressed and heat treated at 1200℃ for 1hour resulted in tetragonal phase transformation while the other 3 samples showed cubic phase determined by XRD data.

Table 6 Compositions chosen to be processed with Hot Isostatic Pressing

Sample	Density(g/cc)
008 Cold Pressed-1200℃ 1 hour	1.7179
008 Cold Pressed-1300℃ 1 hour	1.5129
SPS 001	1.5787
SPS 008	1.8434

CONCLUSION

The results indicate that a homogeneous composition was difficult to achieve from the combination of the three separate powders. The transition from LUDOX silica to TEOS silica did help reduce the phase transformation from cristobalite to the unwanted tridymite phase. The data collected by XRD shows crystalline phase while the TEM images show multiple different phases were present. Also seen in the XRD data, many of the compositions transitioned from β-(cubic) to α-cristobalite (tetragonal) when pulverized verses keeping as a fragmented section. The kinetics for the SiO_2-$AlPO_4$-BPO_4 system can be slow which may lead to the need for longer and higher temperature heat treatments. Higher heat treatments result in the loss of boron in the composition due to boron's vapor pressure which results in a change in the chemical composition. Other results showed that the addition of a small amount of sodium in the LUDOX silica, can result in the phase transformation from β-cristobalite to tridymite.

FUTURE WORK

For this project, there are still processes to be analyzed and improved in the future work. One aspect to improve, is to determine a process to create amorphous BPO_4, and $AlPO_4$ and intimate mixing between the three constituents. Also, research other

techniques that may create a more dense and transparent material along with other ways to stabilize the β-cristobalite phase at room temperature. Since the compositions transition so easily during grinding, the composition stability needs to be improved to prevent further transitions upon analysis preparations.

REFERENCES

[1] Ceramics Working Group, "Microstructure and properties," University of Chemistry and Technology, Prague, 2004. [Online].

[2] "Transparent Ceramics: CoorsTek Corporation." *Transparent Ceramics | CoorsTek Corporation*, www.coorstek.co.jp/eng/rd/detail_04.html.

[3] J. B. Wachtman, W. R. Cannon, and M. J. Matthewson, Mechanical Properties of Ceramics, Second Editon. 2009.

[4] W. D. Callister, "Materials science and engineering: An introduction (2nd edition)," Mater. Des., 1991.

[5] Childs, P.E. "Chemical Bonding and the Structure and Properties of Materials." RACI Chem Ed Central, 5 Mar. 2018, racichemedcentral.com.au/ancq/ancq-chemical-resources/chemical-bonding-and-the-structure-and-properties-of-materials.

[6] H. E. Bergna, "Colloid Chemistry of Silica," Adv. Chem. ACS, vol. 126, no. 3173, pp. 273–273, 1930.

[7] "Solid State Structure." NDT Resource Center, www.nde-ed.org/EducationResources/CommunityCollege/Materials/Structure/solidstate.htm.

[8] W. D. Kingery, "Introduction to Ceramics," J. Electrochem. Soc., 2006.

[9] Buerger, M. J. "The Stuffed Derivatives of the Silica Structures." Vol. 15, 1947, pp. 600–614.

[10] T. Demuth, Y. Jeanvoine, J. Hafner, and J. G. Ángyán, "Polymorphism in silica studied in the local density and generalized-gradient approximations," J. Phys. Condens. Matter, vol. 11, no. 19, pp. 3833–3874, 1999.

[11] Smith, Deane K. "Opal, Cristobalite, and Tridymite: Noncrystallinity versus Crystallinity, Nomenclature of the Silica Minerals and Bibliography." Powder Diffraction, vol. 13, no. 1, Mar. 1998, pp. 2–19., doi:10.1017/s0885715600009696.

[12] "Fused Quartz." *Wikipedia*, Wikimedia Foundation, 17 Nov. 2020, en.wikipedia.org/wiki/Fused_quartz.

[13] Gibbs, R. E. "The Polymorphism of Silicon Dioxide and the Structure of Tridymite." *The Royal Society Publishing*, vol. 113, no. 764, pp. 351–368.

[14] "Developments in Geochemistry," Dev. Geochemistry, 1991

[15] D. Hillel, Encyclopedia of soils in the environment. 2004.

[16] C. Topics et al., "Overview of Silica Polymorphs The Quartz Page : The Silica Group The Silica Group Dependence of Structure on Temperature," vol. 067, pp. 1–15, 2015.

[17] N. R. Keskar and J. R. Chelikowsky, "Structural properties of nine silica polymorphs," Phys. Rev. B, vol. 46, no. 1, pp. 1–13, 1992.

[18] Shelton, Hannah, et al. "The Ideal Crystal Structure of Cristobalite XI: A Bridge in SiO2 Densification." *The Journal of Physical Chemistry*, vol. 122, 2018, pp. 17437–17446., doi:10.1021/acs.jpcc.8b04282.s001.

[19] "Crystallography III, X-Ray Diffraction." Geo Arizona, www.geo.arizona.edu/xtal/geos306/geos306-11.htm.

[20] Hu, Yung-Haw, et al. *Boron Aluminum Phosphates and Boron Aluminum Phosphosilicates for Electronic Packaging*. 23 Jan. 1992.

[21] Unknown. “Devitrification.” *Encyclopedia Britannica*, 27 Nov. 2014, www.britannica.com/science/devitrification.
[22] Fleming, J. D. “FUSED SILICA MANUAL.” *Georgia Institute of Technology*, 1964, pp. 1–152.
[23] Rok, Task. “QUARTZ, FUSED QUARTZ, FUSED SILICA, WHAT'S THE DIFFERENCE?” *Highlyeducatedti.com*, 27 Sept. 2018, highlyeducatedti.com/blogs/information/quartz-fused-quartz-fused-silica-whats-the-difference?
[24] LUDOX TM-50 colloidal silica-50 wt.% suspension in H_2O. 420778. Spec sheet. Sigma-Aldrich. 18 APR 2013.
[25] Wang, Xiao-Dong, et al. “Preparation of Spherical Silica Particles by Stober Process with High Concentration of Tetra-Ethyl-Orthosilicate.” *Journal of Colloid and Interface Science*, vol. 341, no. 1, 2010, pp. 23–29., doi:10.1016/j.jcis.2009.09.018.
[26] Kmecl, Primoz, and Peter Bukocec. “Boron Phosphate: Its Synthesis, Gradual Crystallization and Characterization of Bulk Properties.” *Acta Chimica Slovenica*, vol. 46, no. 2, 19 May 1998, pp. 161–171., doi:10.1107/s0108768107031758/bs5044sup1.cif.
[27] “NEW PELCO® Tripod Polisher™ 590TEM, 590SEM, 590TS.” *PELCO Tripod Polisher™ 590*, www.tedpella.com/Material-Sciences_html/PELCO-Tripod-Polisher-590.htm.
[28] “Ion Milling.” *Nanoscience Instruments*, 2 Aug. 2018, www.nanoscience.com/techniques/ion-milling/.
[29] “Zero Diffraction Plate for XRD.” *Silicon Crystal Sample Holders - Sil'tronix Silicon Technologies*, www.sil-tronix-st.com/en/optical-products/zero-diffraction-plate.
[30] “X-Ray Powder Diffraction (XRD).” *Techniques*, 14 Feb. 2020, serc.carleton.edu/research_education/geochemsheets/techniques/XRD.html.
[31] “Crystal Twinning.” *Wikipedia*, Wikimedia Foundation, 18 Nov. 2020, en.wikipedia.org/wiki/Crystal_twinning.
[32] Davis, R. F. “Hot Isostatic Pressing.” *Concise Encyclopedia of Advanced Ceramic Materials*, 1991, pp. 210–215., doi:doi.org/10.1016/B978-0-08-034720-2.50061-7.
[33] Werr, Ulrich. “Porous Ceramics Manufacture – Properties – Applications.” *Technology Insights*, vol. 2, 2014, pp. 48–52.
[34] “Spark Plasma Sintering.” *Wikipedia*, Wikimedia Foundation, 3 Oct. 2020, en.wikipedia.org/wiki/Spark_plasma_sintering.